UNIVERSIDAD NACIONAL DE INGENIERÍA

FACULTAD DE CIENCIAS

TESIS

" AN ALGORITHM OF FEASIBLE DIRECTIONS TO MIXED NONLINEAR COMPLEMENTARITY PROBLEMS AND APPLICATIONS "

PARA OBTENER EL GRADO DE DOCTOR EN
CIENCIAS CON MENCIÓN EN MATEMÁTICA

ELABORADO POR
Ramírez Gutiérrez, Angel Enrique

ASESOR
DR. ELADIO OCAÑA ANAYA
CO–ASESOR
DR. GRIGORI CHAPIRO

LIMA–PERÚ
2017

Dedication

This dissertation is lovingly dedicated to my mother, Graciela América Gutiérrez de Ramírez. Her support, encouragement and constant love for her family are example of life for me. To my father Angel Ramírez, for all your support and love.

Acknowledgements

I am very thankful to everyone and sincerely sorry for all those who are not cited here explicitly. First I would like to thank my advisor Dr. Eladio Ocaña Anaya by his trust to my person, his sugestions and advises in this difficult work. Also, I would like to thank my co-advisor Dr. Grigori Chapiro for the support during all my time at Universidade Federal de Juiz de Fora and his help, valuable advise and suggestions he gave me. I thank to Dr. Sandro Mazorche of Universidade Federal de Juiz de Fora for help me when I did not understand the ideas about of algorithm. For everyone, thanks by yours friendship.

I thank my daughter Angely, my wife Luz María and my parents by theirs support and for accepting that I dedicated much less time to them during my doctoral studies. I thank all my friends of doctoral program as Luis, Hugo, Ernesto, Helmut, Julio and all colleagues at IMCA. I thank also to Eliza Ferreira, Gisele Texeira and Daniel Pereira, i met them at Universidade Federal de Juiz de Fora. Their helps was important during my studies.

I would like to thank all my professors at IMCA for everything I learned during these years and IMCA's staff for the excellent and incomparable support. I thank to Laboratorio de Simulación e Investigación Numérica and its director Dra. Irla Mantilla, place where I gave my first steps as researcher. Finally, I thank the FONDECYT by its program "Generación Científica - Becas Nacionales - Fortalecimiento de Programas de doctorado en universidades peruanas" under award 217-2014 for the financial support during these years.

Table of Contents

List of Tables

List of Figures

Abstract

This work investigates the Feasible Direction Algorithm using interior points applied to the Mixed Nonlinear Complementarity Problem and some applications. This algorithm is based in Feasible Directions Algorithm for Nonlinear Complementarity Problem, which is described briefly. The proposed algorithm is important because many mathematical models can be written as mixed nonlinear complementarity problem. The principal idea of this algorithm is to generate, at each iteration, a sequence of feasible directions with respect to the region, defined by the inequality conditions, which are also monotonic descent directions for one potential function. Then, an approximate line search along this direction is performed in order to define the next iteration. Global and asymptotic convergence properties for the algorithm are proved. In order to validade the robustness the algorithm is tested on several benchmark problems, that were found in the literature, considering the same parameters. In this work one dimensional models describing Oxygen Diffusion inside one cell and In Situ Combustion are also presented together with bidimensional model of the Elastic–Plastic Torsion Problem. These models are re-written as nonlinear complementarity problem and mixed nonlinear complementarity problem. These new formulations are discretized by Finite Diference Scheme or Finite Element Method and, for its discrete forms, the algorithm will be applied. The numerical results are compared with direct numerical simulation using Newton's method (in the case of Oxygen Diffusion and In Situ Combustion) or exact solution (in the case of Elastic–Plastic Torsion Problem). It is shown that the obtained results are in good agreement with the asymptotic analysis. For the In situ combustion model the corresponding Riemann's problem is studied in order to validate numerical solutions.

Resumen

Este trabajo investiga el Algoritmo de Direcciones Factibles para Problemas de Complementaridad no Lineal Mixta y algunas aplicaciones. Este algoritmo está basado en el Algoritmo de Direcciones Factibles para Problemas de Complementaridad no Lineal, el cual es descrito brevemente. El algoritmo propuesto es importante porque muchos modelos matemáticos pueden ser escritos como problemas de complementaridad no lineal mixta. La idea principal de este algoritmo es generar, en cada iteración, una sucesión de direcciones factibles con respecto a la región, definida por las condiciones de desigualdades, los cuales son direcciones descendentes monótonas para una función potencial. Posteriormente, una búsqueda lineal a lo largo de esta dirección es realizada con el fin de obtener el nuevo punto e iniciar la siguiente iteración. Propiedades de convergencia global y asintótica son probados. Con el fin de validar la robustez del algoritmo, éste es testeado sobre varios problemas testes encontrados en la literatura, considerando los mismos parámetros. Se presentan modelos unidimensionales describiendo la Difusión de Oxígeno dentro de una célula y el proceso de Combustión In Situ junto con un modelo bidimensional del Problema de Torsión Elasto-Plástico. Estos modelos son reescritos como problemas de complementaridad no lineal y no lineal mixta. Estas nuevas formulaciones son discretizadas usando el Esquema de Diferencias Finitas o el Método de Elementos Finitos y, para sus formas discretas, el algoritmo será aplicado. Los resultados numéricos son comparados con simulación numérica directa usando el Método de Newton (en el caso de Difusión de Oxígeno y Combustión In Situ) o la solución exacta (en el caso del problema de Torsión Elasto-Plástico). Es mostrado que los resultados obtenidos concuerdan con el análisis asintótico. Para los modelos de Combustión In Situ el respectivo problema de Riemann es estudiado con el objetivo de validar nuestras soluciones numéricas.

INTRODUCTION

There are many problems in Engineering, Economics and other fields of science that can be formulated as mixed nonlinear complementarity problems (MNCP), [1, 2]. This kind of problems is very interesting from the point of view of optimization and modeling, even more, it is very difficult find the exact solution. Between the several problems, in this work it is briefly presented in situ combustion (ISC) process, which is a very important technique to heavy oil extraction and there is a renewed interest in heavy oil recovery techniques. In particular, in north weast of Peru there exists heavy oil in Cuenca del Marañón, as it is showed in Figure 1.

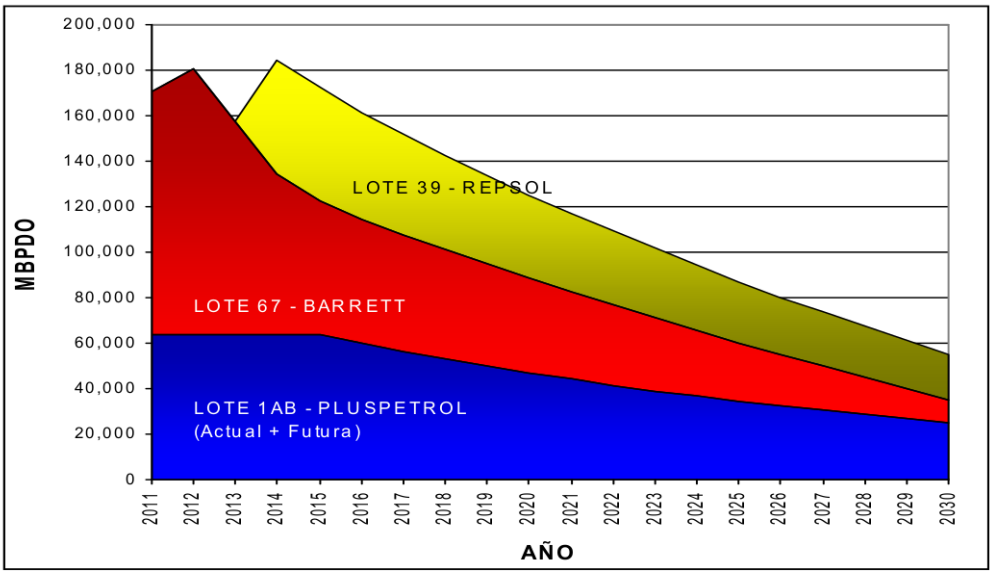

Figure 1: Projection of heavy oil reserves. Source: INGEPET–2008, [3].

This technique basically consists in the injection of air, pure oxygen or air enriched with oxygen to enable the combustion within of reservoir. It allows the release of heat, which is conducted ahead of the combustion front, thus reducing the high oil

viscosity. A limitation of ISC is that the combustion front is hard to control and there are few mathematical models for that. The models normally are systems of nonlinear partial differential equations and their solutions are very difficult to be calculated. This difficulty supports the research interest in this subject in different areas such as Engineering, Physics, Computer Science and Mathematics, [4].

Another interesting problem is the Elastic–Plastic Torsion Problem. There exists many publications about this problem as in [5] it is studied as nonlinear boundary value problem, in [6] is proposed as variational inequalities and it is solved by a computational procedure based on the subgradient method. On the other hand, the application of mathematical programming theory and methods, including complementarity to analyze elastic-plastic structures dates back to the late 1960s and early 1970s. Obstacle problems leading to MNCP are less studied in the form of the complementarity problems [7]. Torsion of a long, hollow bar made of an elastic-plastic material is a mathematically well-defined problem [8] and thus it can be used to test the proposed algorithm.

All the models described in this work are of the kind of free boundary problem and for approximating the analytical solutions have been developed many algorithms of interior points and feasible directions (FDA). In this direction is presented a algorithm of feasible directions for mixed nonlinear complementarity problems (FDA–MNCP). An advantage of this formulation is that no free boundaries are present. For example, Elastic-Plastic Torsion Problems [9, 10] can be modeled as free boundary problems and can be written as mixed complementarity problem [11]. Another example involves an in-situ combustion described by a system of two nonlinear differential equations, this has been modeled as a Complementarity Problem [12] or Mixed Complementarity Problem [13]. Other examples can be found in [2].

A lot of papers aim at providing a numerical solution of MNCP. These include works using the interior point methods [14], non monotone stabilization scheme [15], a class of active set Newton's methods [16, 17], fictitious time integration methods [18], hy-

brid smoothing method [19], among others [20]. In this work Feasible Directions Algorithm (FDA) is employed to solve MNCP. This method consists of an interior point algorithm based on a modification of Newton's method characterized by fast convergence, easy computational implementation and robustness. The present method deals with inequality constraints and complementarity conditions in a way inspired by an algorithm for constrained optimization presented in [21, 22, 23]. This approach, as in primal dual algorithms, solves optimality conditions with Newton-like iterations. However, the iterations are perturbed in such a way to have feasible descent directions. At each iteration one feasible descent search direction is computed by following the ideas of FDA–NCP [24]. The presented algorithm is appropriate for practical applications since it brings together the classical numerical techniques for PDEs combined with a robust and efficient interior point algorithm for MNCP, which has a complete theoretical foundation and shows good numerical results. The first steps in this direction were given by Mazorche in [25].

This work is organized as follows. In Chapter 1 is briefly presented a description of a model about the diffusion of oxygen into absorbing tissue, which considers a linear model and that was first studied in [26]. In order to consider more general models for diffusion of oxygen, two models about in situ combustion process are considered. They consist of systems of nonlinear partial differential equations and these models have a strong nonlinearity because it considers the Arrhenius's law in the source term. In the end, it is briefly described the Elastic-Plastic Torsion Problem and its formulation as free boundary problem, where we want to found the boundary that separates the elastic and the plastic parts.

In Chapter 2 is presented briefly the Feasible Direction Algorithm for Nonlinear Complementarity Problem (FDA–NCP), which is completely developed in [24]. The model of Diffusion of Oxygen and In Situ Combustion are rewritten as NCP.

In Chapter 3, we present several forms to define Mixed Nonlinear Complementarity Problem (MNCP) and the Feasible Directions Algorithm for MNCP, which is called

(FDA–MNCP). This algorithm is an adaptation of FDA–NCP for MNCP and its theoretical properties are proved including the properties on global and asymptotic convergence. FDA–MNCP is applied to solve benchmark problems found in the literature showing the convergence and robustness. In this section the models about In Situ Combustion and Elastic–Plastic Torsion Problem are formulated as MNCP.

In Chapter 4, we consider the discrete formulation of models described in Chapter 2 and Chapter 3. To obtain the discrete formulation it is used the Crank–Nicolson's Finite Difference Scheme, see [27] or Finite Element Method, see [28]. After, we describe an scheme such that FDA–NCP, FDA–MNCP can be used to solve the discrete problem at each time step for evolutive problems.

Finally, in Chapter 5 we present some conclusions and also some proposals for a future work.

Chapter 1

THEORICAL FRAMEWORK

In this section, four math models are briefly described, for each one are showed the governing equations. The first model corresponds to Diffusion of Oxygen, the next two models corresponds to in situ combustion model and the fourth model is related to Elastic–Plastic Torsion Problem. These models are interesting since they correspond to free boundary problems, thus is very difficult to find the analytical solution. These models are formulated as NCP in Chapter 2 and as MNCP in Chapter 3. The discrete formulations using finite difference esqueme for In Situ Combustion are done in Appendix A and for Elastic–Plastic Torsion Problem is done in Section 3.6 using finite element method.

1.1 The oxygen diffusion problem

Here is studied the particular case of one dimensional oxygen diffusion that involves a moving boundary. For simplicity, the oxygen is allowed to diffuse into a medium that consumes oxygen at constant rate. The concentration of oxygen at the surface of the medium is kept constant. A moving boundary marks the limit of oxygen penetration.

The major challenge is that of tracking the movement of the boundary during this stage of the process as well as determining the distribution of oxygen throughout the medium at any instant. This type of problem is known as an implicit moving bound-

ary problem; see [29]. Several analytical and numerical methods were employed to solve this problem. We mention [26, 30, 31, 32, 33, 34, 35] and references therein.

The process takes place in two phases. The first one evolves until a steady state without oxygen transfer into the medium is attained. At the second phase the surface of the medium is sealed so that no more oxygen passes in or out. The medium continues to consume the oxygen in it already diffusing in it and, as a consequence, the boundary marking the depth of penetration in the steady state recedes towards the sealed surface.

Following [29, 36], the system of partial differential equations describing this problem can be written in non-dimensional form:

$$\frac{\partial c}{\partial t} = \frac{\partial^2 c}{\partial x^2} - 1, \quad 0 \leq x \leq s(t), \tag{1.1}$$

$$\frac{\partial c}{\partial x} = 0, \quad x = 0, \quad 0 < t, \tag{1.2}$$

$$c = \frac{\partial c}{\partial x} = 0, \quad x = s(t), \quad 0 < t, \tag{1.3}$$

$$c = \frac{1}{2}(1 - x)^2, \quad 0 \leq x \leq 1, \quad t = 0, \tag{1.4}$$

where $c(x, t) \geq 0$ is the concentration of oxygen free to diffuse and $s(t)$ is the value of x separating regions where $c = 0$ and $c > 0$. Eq. (1.1) represents the PDE at the left side of the moving boundary, Eqs. (1.2) and (1.3) represent the boundary conditions and Eq. (1.4) is the initial condition.

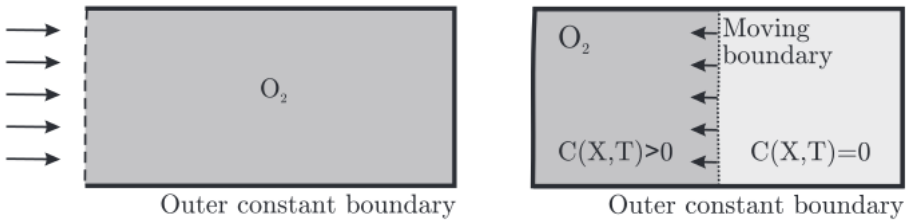

Figure 1.1: Schematic representation of the oxygen diffusion into the media sample. The first stage is represented on the left. Here the oxygen enters the sample until equilibrium is reached. During the second phase, on the right, the sample is sealed and the oxygen inside diffuses and is absorbed by the medium generating the moving boundary, [37, 36].

1.2 In situ combustion models

The process of In Situ Combustion are applied in heavy oil reserves. It consists in the injection of compressed air inside of reservoir to permite the combustion of oil components. The heat and transport of the energy allows that obtain carbon, combustion gas, light oil and others components. This technique allows decrease the oil viscosity, it is very important in the oil recuperation. Besides, one caracteristic this technique is its fast kinetics, removing the costs and disadvantages of generate energy on the surface, has the advantage that the oil resulting can be improved partially and the combustion gas remain inside of reservoir, [38, 39, 40]. Figure 1.2 shows the different zone in the process of in situ combustion.

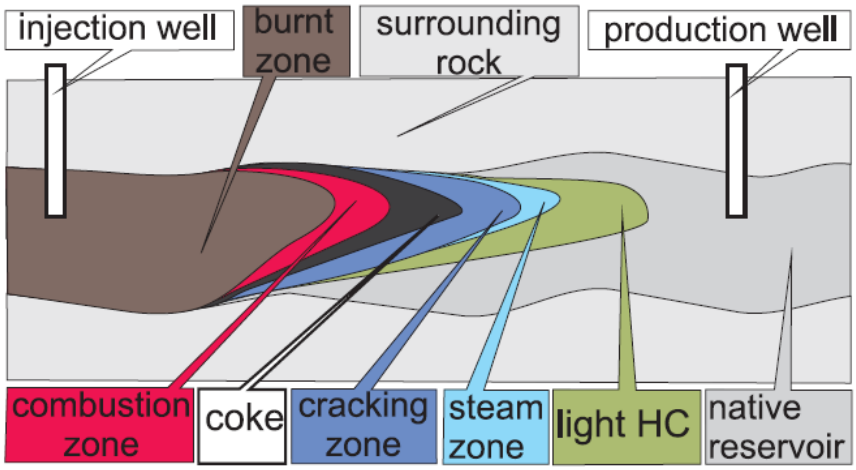

Figure 1.2: Process of in situ combustion, [4].

One difficult in this process is to obtain information about combustion front, which is present in travelling wave form. The models describe in this section can help in give information about combustion front. Majors details on models describe in this section can see in [4, 41].

1.2.1 Model 1

This is the simplest model and it consists of a system of two nonlinear differential equations, derived from [42, 43], which solution possesses multiple scales and it was studied theoretically in [12].

In this model, see [36], is considered that only a small part of the available space is occupied by the fuel, so that changes of porosity in the reaction are negligible. We assume that pressure variations are small compared to prevailing pressure yielding constant gas speed and local thermal equilibrium i.e., the temperatures of solid and gas are the same. Heat losses are neglected, which is reasonable for in-situ combustion in field conditions. We consider unlimited supply of oxygen. In dimensionless form the simplified model is written

$$\frac{\partial\theta}{\partial t} + u\frac{\partial(\rho\,\theta)}{\partial x} = \frac{1}{Pe_T}\frac{\partial^2\theta}{\partial x^2} + \Phi, \tag{1.5}$$

$$\frac{\partial\eta}{\partial t} = \Phi, \tag{1.6}$$

$$\rho = \frac{\theta_0}{\theta+\theta_0}, \tag{1.7}$$

$$\Phi(\theta,\eta) = \beta(1-\eta)exp\left(-\frac{\mathcal{E}}{\theta+\theta_0}\right), \tag{1.8}$$

where θ is the scaled temperature, η represents immobile fuel depth as commonly used in oil engineering ($\eta = 1$ means no fuel and $\eta = 0$ means maximum fuel). Here Pe_T is the Peclet number for thermal diffusion, u is the dimensionless gas speed, $\mathcal{E}$ is the scaled activation energy and θ_0 is the scaled reservoir temperature. The system must be solved with the initial reservoir conditions

$$t = 0,\ x \geq 0: \quad \theta = 0, \quad \eta = 0,$$

and the left boundary conditions corresponding to the injection conditions

$$t \geq 0,\ x = 0: \quad \theta = 0,\ \eta = 1.$$

1.2.2 Model 2

This is a simple model and it consists of a system of three nonlinear differential equations, analogous to model presented in [41, 44, 45]. The model consists of the heat balance equation given by Equation (1.9), which represents transport and diffusion of heat and production of heat in the chemical reaction; the oxygen balance equation given by Equation (1.10), which represents transport and consumption of oxygen;

the immobile fuel balance equation given by Equation (1.11), which represents consumption of the solid fuel:

$$\frac{\partial \theta}{\partial t} + V_T \frac{\partial \theta}{\partial x} = \frac{1}{Pe} \frac{\partial^2 \theta}{\partial x^2} + \mu_T \Phi(\theta, Y, \eta), \tag{1.9}$$

$$\frac{\partial Y}{\partial t} + V_Y \frac{\partial Y}{\partial x} = \lambda_Y \frac{\partial^2 Y}{\partial x^2} - \mu_Y \Phi(\theta, Y, \eta), \tag{1.10}$$

$$\frac{\partial \eta}{\partial t} = -\mu_\eta \Phi(\theta, Y, \eta), \tag{1.11}$$

where

$$\Phi(\theta, Y, \eta) = Y \eta \exp\left(-\frac{\mathcal{E}}{\theta + \theta_0}\right). \tag{1.12}$$

Here V_T and V_Y are thermal and oxygen transport speeds and is assumed that oxygen is transported faster than temperature, i.e. $V_Y > V_T > 0$, which is physically realistic in rock porous media since the thermal capacity of the gas is smaller than the thermal capacity of the porous medium. The term Φ represents the reaction rate and, differently from [41, 44], here is considered the complete Arrhenius law given by Equation (1.12). The constant λ_Y is the oxygen diffusion, $\mathcal{E}$ is the scaled activation energy, θ_0 is the scaled reservoir temperature, μ_T, μ_Y and μ_η represent the dimensionless quantities of temperature, oxygen consumed and fuel during the reaction. Constant Pe represents the Peclet's number.

The System (1.9)–(1.11) is solved using the following constant boundary conditions

$$\theta(0,t) = \theta_L,\ Y(0,t) = Y_L,\ \eta(0,t) = \eta_L, \quad \forall\, t \geq 0,$$

$$\theta(\infty,t) = \theta_R,\ Y(\infty,t) = Y_R,\ \eta(\infty,t) = \eta_R, \quad \forall\, t \geq 0,$$

1.3 Elastic–plastic torsion problem

Following [46, 47] a prismatic bar whose longitudinal axis is the Z-axis and whose cross sections Ω lie in the XY-plane is considered, see Figure 1.3.

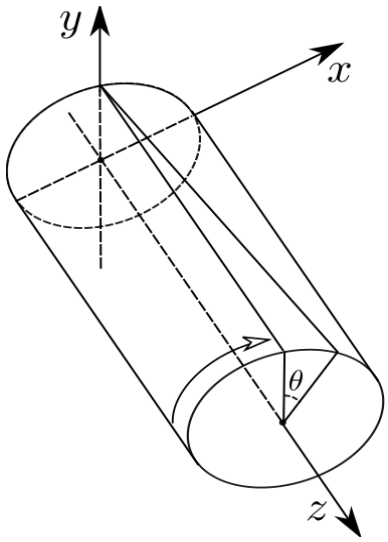

Figure 1.3: Torsion of a prismatic bar with circular cross section.

The Saint-Venant theory assume that the displacements in the x, y, and z directions, respectively, are given by

$$u = -yz\theta, \quad v = xz\theta, \quad w = w(x, y, \theta),$$

where θ is the angle of twist per unit length and $w(x, y, \theta)$ denotes the warping function, which is directly proportional to the angle of twist per unit length θ in the elastic case. For the plasticity problem this is, in general, no longer true, see [47]. Except for the circular cross section case, there are no analytical solutions available, [8].

That is why, in the present paper the circular cross sections is considered corresponding to $w = 0$, see [46, 48]. Following [10], it is assumed $\Omega \subset \mathbb{R}^2$ as a simply connected, bounded open domain and a cylindrical bar with cross-section Ω made of an elastic plastic material. This elastic-plastic torsion problem is described by the system of equations in terms of a stress function ϕ, see [10, 49],

$$\begin{aligned} \phi &= 0 \text{ on } \partial\Omega; \\ -\nabla\phi &= \theta \text{ in } \Omega_e = \{x \,/\, x \in \Omega, |\nabla\phi| < 1\}; \\ |\nabla\phi| &= 1 \text{ in } \Omega_p = \Omega - \Omega_e, \end{aligned} \tag{1.13}$$

where Ω_e is the elastic region, Ω_p is the plastic region and θ is the twist angle per unit length.

Chapter 2

NONLINEAR COMPLEMENTARITY PROBLEM

In this chapter is presented the Feasible Directions Algorithm for Nonlinear Complementarity Problem (FDA–NCP), which is a perturbation of Newton's method. The basic idea is generating a feasible direction for a domain Ω and that direction is a descent direction for some potential function. This algorithm is studied in detail in [24]. It is important because parabolic problems can be written as a variational problem involving a complementarity condition and moving boundaries, and these appear in several applications; see [29]. In [1] several examples in Engineering and Economics are described. In [24, 36] is proposed a general technique for moving boundary problems, that can be written as the complementarity problem, and implement it for the one dimensional case.

The numerical method is based on a combination of the Crank-Nicolson finite difference scheme, [27], and a globally convergent nonlinear complementarity algorithm (FDA-NCP), [50]. As a result the moving boundary is obtained naturally, without need of regularizations unlike from other methods. The robustness of the algorithm allows longer time steps as shown in our preliminary results; see [36]. Other methods dealing with complementarity problems can be found in [50, 51, 52, 53]. The present

technique is appropriate for practical applications since it brings together classical numerical techniques for PDEs with a robust and efficient interior point algorithm for nonlinear complementarity problems, having a complete a theoretical fundamentation and good numerical results. Finally, the models described in Chapter 1 are written as NCP and then are solved by FDA–NCP in Chapter 4.

2.1 The numerical method

In this section, we describe our approach to solve the system of parabolic partial differential equations numerically The problem consists in finding $u(x,t) : I \times \mathbb{R}_+ \to \mathbb{R}^n$ and the moving boundary $s(t) : \mathbb{R}_+ \to \mathbb{R}$ such that

$$F(u) = 0, \quad \text{for } x < s(t); \quad \text{and} \quad u = 0, \quad \text{for } x \geq s(t), \tag{2.1}$$

where $F(u) : \mathbb{R}^n \to \mathbb{R}^n$ and the interval I can be $\mathbb{R}$, $\mathbb{R}_+$ or a compact interval. We study the case when Eq. (2.1) can be written as the complementarity problem using Hadamard product "$\bullet$",

$$F(u) \geq 0, \quad u \geq 0 \quad \text{and} \quad u \bullet F(u) = 0. \tag{2.2}$$

Several examples where (2.1) and (2.2) are equivalent can be found in [54].

We use FDS and FEM for space discretization and a Nonlinear Complementarity Algorithm to solve the discrete problem at each time step. In this way the implementation is flexible, since we can change the space discretization and the algorithm independently. Next we present a brief description of the algorithm FDA-NCP.

2.1.1 The nonlinear complementarity algorithm

Let $F : D \subset \mathbb{R}^n \to \mathbb{R}^n$ be a nonlinear vector function and continuously differentiable. The nonlinear complementarity problem (NCP) consists in finding $x \in \mathbb{R}^n$ satisfying (2.2), where $x \geq 0$ means that each component of the vector x is nonnegative. The set $\Upsilon = (x \in \mathbb{R}^n \ : \ x \geq 0, \, F(x) \geq 0)$ is called the feasible set and $\text{int}(\Upsilon)$ its interior.

FDA-NCP is an iterative algorithm to solve problem (2.2). It starts from an initial point in int(Υ) and generates a sequence of points also in int(Υ) that converges to the required solution. At each point it defines a feasible direction, that is also a descent direction for the potential function $\Phi(x) = \sum_{i=1}^{n} x_i\, F_i(x)$. On that direction a new interior point with a lower potential is obtained. This point is defined to be the next point of the sequence and the algorithm returns to the first step till a convergence criterion is satisfied. The search direction is based on Newton's direction for the nonlinear system of equations $x \bullet F(x) = 0$. To obtain feasibility, Newton's direction is modified by a restoration direction, as done in [21]. The geometric interpretation can be observed in Figure 2.1.

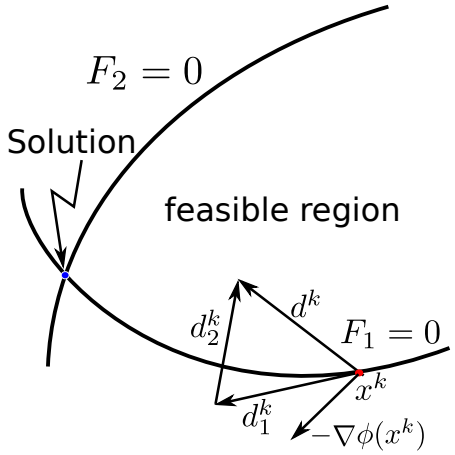

Figure 2.1: Direction d^k is generated by FDA–NCP. It is based in Newton's direction d_1^k and a restoration direction d_2^k.

2.2 Description of the algorithm FDA–NCP

The following notation will be employed to describe the algorithm FDA-NCP:

$$
\begin{aligned}
&F^k = F(x^k),\\
&\Phi^k = \Phi(x^k),\\
&M^k = \nabla(x^k \bullet F(x^k)), \quad \text{and}\\
&\nabla\Phi^k = \nabla\Phi(x^k)
\end{aligned}
$$

Algorithm 1: FDA–NCP

Parameters: $E = [1, ..., 1]^T \in \mathbb{R}^n$, $\nu, \nu_1 \in]0, 1[$, $\alpha \in]0, 1/2[$, $\rho_0\, c^{\beta-1}(x^k) < 1$.

Data: $x^0 \in \text{int}(\Upsilon)$, $k = 0$. Tolerancia

Result: x^k as a solution aproximate of NCP.

initialization;

$k \leftarrow 0$;

while $|\Phi(x^k)| >$ *Tolerancia* **do**

Calcule the search direction d^k resolving the system

$$M^k\, d^k = -x^k \bullet F^k + \alpha\, \rho^k\, E.$$

where $\rho^k = \rho_0 \frac{\phi^\beta(x^k)}{n}$.

Armijo line search. Set t^k as the first number in the sequence $1, \nu, \nu^2, \nu^3, ...$ that satisfies:

$$x^k + t^k\, d^k \geq 0, \tag{2.3}$$

$$F(x^k + t^k\, d^k) \geq 0, \tag{2.4}$$

$$\Phi(x^k + t^k\, d^k) \geq \Phi^k + t^k\, \nu_1\, (\nabla\Phi^k . d^k). \tag{2.5}$$

Update. Set $x^{k+1} = x^k + t^k\, d^k$.

$k \leftarrow k + 1$

end while

Output: $\boldsymbol{x}^k$ is a aproximate solution of NCP.

In [24, 21] it has been shown that the search direction d^k is well defined in Υ and the global convergence of FDA-NCP scheme is guaranteed under the following assumptions:

Assumption 2.2.1. *The set* $\Upsilon_c = \{x \in \Upsilon : \Phi(x) < c\}$, $c > 0$ *is a compact set and has an interior* Υ_c^0. *Each* $x \in \Upsilon_c^0$ *satisfies* $x > 0$ *and* $F(x) > 0$.

Assumption 2.2.2. *The function* F *is continuously differentiable and* $\nabla F(x)$ *satisfies the Lipschitz condition* $||\nabla F(w) - \nabla F(u)|| < \gamma_0 ||w - u||$, *for any* u, $w \in \Upsilon_c$, *where* γ_0 *is a positive real number.*

Assumption 2.2.3. *The matrix* $diag(F(x)) + diag(x)\,\nabla F(x)$ *has an inverse in* Υ_c^0.

The FDA–NCP is supported by strong theoretical results and with Assumptions 2.2.1–2.2.3 are proved the next theorems in [24].

Theorem 2.2.1. *Given an initial feasible point* $x^0 \in \Upsilon_c$, *the sequence* $\{x^k\}$ *generated by FDA–NCP converges to* x^*, *a solution of nonlinear complementarity problem.*

Theorem 2.2.2. *Consider the sequence* $\{x^k\}$ *generated by the FDA–NCP, that converges a solution* x^* *of nonlinear complementarity problem. Then:*

i) Taking $\beta \in]1, 2[$ *and* $t^k = 1$ *for* k *large enough, then the rate of convergence of FDA–NCP is at least superlinear.*

ii) If $t^k = 1$ *for* k *large enough and* $\beta = 2$, *then the rate of convergence of FDA–NCP is quadratic.*

2.3 Oxygen diffusion formulated as NCP

Following [26], System (1.1)-(1.4) can be rewritten into a variational formulation in the form of Eq. 2.2.

$$\begin{aligned} & c \geq 0, \\ & \frac{\partial c}{\partial t} - \frac{\partial^2 c}{\partial x^2} + 1 \geq 0, \\ & \left(\frac{\partial c}{\partial t} - \frac{\partial^2 c}{\partial x^2} + 1\right) c = 0, \end{aligned} \tag{2.6}$$

where the boundary and the initial conditions are defined by (1.2) and (1.4) respectively. The first inequality in (2.6) is satisfied as equality by (1.1) inside the region $0 < x < s(t)$. When $s(t) \leq x \leq 1$ by (1.3) we get $c = 0$ and thus (2.6) is valid. The inequality $c \geq 0$ follows from (1.4). The equality in (2.6) is valid because for any $x \in [0, 1]$ one of the factors vanishes.

The equivalence between the solution of the system of equations in the variational approach (2.6) and the weak solution of the Stefan problem described by the system (1.1)-(1.4) was locally studied in [55] and [56].

2.4 In situ combustion models formulated as NCP

2.4.1 Model 1

In order to represent the System (1.9)-(1.11) in a nonlinear complementarity problem we make a transformation similar to Section 2.3 (see also [51]), obtaining:

$$\begin{aligned} &\theta \geq 0; \quad \eta \geq 0; \\ &\frac{\partial \theta}{\partial t} + u\frac{\partial(\rho\theta)}{\partial x} - \frac{1}{\mathrm{Pe}_T}\frac{\partial^2\theta}{\partial x^2} + \Phi \geq 0; \\ &\frac{\partial \eta}{\partial t} - \Phi \geq 0; \end{aligned} \tag{2.7}$$

$$\begin{aligned} &\left(\frac{\partial \theta}{\partial t} + u\frac{\partial(\rho\theta)}{\partial x} - \frac{1}{\mathrm{Pe}_T}\frac{\partial^2\theta}{\partial x^2} + \Phi\right)\theta = 0; \\ &\left(\frac{\partial \eta}{\partial t} - \Phi\right)\eta = 0. \end{aligned} \tag{2.8}$$

We need Eq. (2.8) to be satisfied at the right end of the interval, where Eq. (1.9) may not be satisfied. This explains the choice of dimensionless variable η describing fuel depth inside the reservoir.

2.4.2 Model 2

A similar transformation done in Section 2.3 and Section 2.4.1 and following [12, 13, 51] in order of written System (1.9)-(1.11) as a nonlinear complementarity problem, is written

$$\theta,\ Y,\ \eta \geq 0: \quad \frac{\partial \theta}{\partial t} + V_T\frac{\partial \theta}{\partial x} - \frac{1}{Pe}\frac{\partial^2\theta}{\partial x^2} - \mu_T\Phi(\theta, Y, \eta) \geq 0, \tag{2.9}$$

$$\frac{\partial Y}{\partial t} + V_Y\frac{\partial Y}{\partial x} - \lambda_Y\frac{\partial^2 Y}{\partial x^2} + \mu_Y\Phi(\theta, Y, \eta) \geq 0, \tag{2.10}$$

$$\frac{\partial \eta}{\partial t} + \mu_\eta\Phi(\theta, Y, \eta) \geq 0, \tag{2.11}$$

The System (2.9)–(2.11) has the complementarity condition

$$\left(\frac{\partial \theta}{\partial t} + V_T\frac{\partial \theta}{\partial x} - \lambda_T\frac{\partial^2\theta}{\partial x^2} - \mu_T\Phi(\theta, Y, \eta)\right)\theta = 0, \tag{2.12}$$

$$\left(\frac{\partial Y}{\partial t} + V_Y \frac{\partial Y}{\partial x} - \lambda_Y \frac{\partial^2 Y}{\partial x^2} + \mu_Y \Phi(\theta, Y, \eta)\right) Y = 0, \tag{2.13}$$

$$\left(\frac{\partial \eta}{\partial t} + \mu_\eta \Phi(\theta, Y, \eta)\right) \eta = 0. \tag{2.14}$$

Chapter 3

MIXED NONLINEAR COMPLEMENTARITY PROBLEM

In [24] is studied the Nonlinear Complementarity Problem (NCP) and is presented a Feasible Directions Algorithm (FDA) to this type of problems, its applications to several test problems and a contact's problem. FDA–NCP was briefly presented in Chapter 2 and for more details see [24]. In [12] this algorithm is applied to In Situ Combustion Model and it present some adventages on Newton's method. There exists in literature some problems as Elastic–Plastic Torsion Problem, [11], that can not written as NCP but that can be written in a more general form. This form is called Mixed Nonlinear Complementarity Problem (MNCP) that is a more general formulation than NCP. Based in FDA–NCP presented in [24, 12], in this section is developed a adaptation of FDA–NCP to MNCP. This new algorithm for MNCP will be denoted by FDA–MNCP. In this section is applied FDA–MNCP to benchmark problems that were obtained of literature. In the end of section are formulated as MNCP the In Situ Combustion Model and Elastic–Plastic Torsion Problem and in Section 4 its numerical solution are obtained by FDA–MNCP. The first steps in this directions were given in [25] and follows the same ideas the direction d^k in Figure 2.1. Similar to FDA–NCP described in [24], we are going to search parameters such that direction d^k become a composition of two directions: a feasible direction to some

set Ω and a descent direction to some potential function f. This results and some applications were published in [57].

3.1 Preliminary definitions

Three different variations of presenting MNCP can be found in the literature.

Definition 3.1.1 ([2, 14, 15]). *Find $x \in \mathbb{R}^n$; $w, v \in \mathbb{R}^n_+$ satisfying*

$$f(x) = w - v, \;\; w^T(x - l) = 0, \;\; v^T(u - x) = 0, \;\; l \leq x \leq u,$$

where $l, u \in \bar{\mathbb{R}}^n = (\mathbb{R} \cup \{-\infty, \infty\})^n$ with $l_i \neq u_i$ for all i and $f : \mathbb{R}^n \to \mathbb{R}^n$ is a continuously differentiable mapping.

Definition 3.1.2 ([11, 19, 20, 58]). *Let $f : \mathbb{R}^n \to \mathbb{R}^n$, f is a continuously differentiable mapping and $l_i, u_i \in \mathbb{R} \cup \{-\infty, \infty\}$, with $l_i < u_i$ for all $i = 1, ..., n$. Find a vector $x \in \mathbb{R}^n$ such that*

$$\begin{aligned} &\text{if } \; x_i = u_i \Rightarrow f_i(x) \leq 0, \\ &\text{if } \; l_i < x_i < u_i \Rightarrow f_i(x) = 0 \;\; \text{and} \\ &\text{if } \; x_i = l_i \Rightarrow f_i(x) \geq 0. \end{aligned}$$

Definition 3.1.3 ([25]). *Find $(x, y) \in \mathbb{R}^n \times \mathbb{R}^m$ such that*

$$\begin{aligned} &x \geq 0, \\ &F(x, y) \geq 0, \\ &Q(x, y) = 0 \;\; \text{and} \\ &x \bullet F(x, y) = 0, \end{aligned} \tag{3.1}$$

where $F : \mathbb{R}^n \times \mathbb{R}^m \to \mathbb{R}^n$ and $Q : \mathbb{R}^n \times \mathbb{R}^m \to \mathbb{R}^m$ are continuously differentiable, $H(x, y) = x \bullet F(x, y)$ represents the Hadamard product

$$H(x, y) = (x_1 F_1(x, y), \; \ldots, \; x_n F_n(x, y))^T.$$

Defs. 3.1.1 and 3.1.2 can be re-written to match Def. 3.1.3 if one considers

$$
\begin{aligned}
F(w,v,x) &= \begin{pmatrix} x_1 - l_1 \\ \vdots \\ x_n - l_n \\ u_1 - x_1 \\ \vdots \\ u_n - x_n \end{pmatrix}, \\
Q(w,v,x) &= f(x) + v - w, \\
\begin{pmatrix} w \\ v \end{pmatrix} &\bullet F(w,v,x) = 0,
\end{aligned}
\tag{3.2}
$$

where $(w, v) \in \mathbb{R}^n_+ \times \mathbb{R}^n_+$ are auxiliary variables and $x \in \mathbb{R}^n$.

Many mathematical programming problems can be formulated as an MNCP. In particular, one can formulate algebraic systems of nonlinear equations by setting $u_i = +\infty$ and $l_i = -\infty$ [20, 58], nonlinear programming can be treated by applying KKT conditions [16, 59], nonlinear complementarity problems by setting $u_i = +\infty$ and $l_i = 0$ [2], Variational Inequalities can be similarly formulated [2, 19].

Considerable research effort was devoted by mathematicians and engineers to solve MNCP, looking for strong and efficient techniques for real engineering applications. Our approach to solve MNCP in the form given by Def. 3.1.3 is based on the iterative solution using Newton's method for the nonlinear system of equations:

$$
S(x,y) = \begin{pmatrix} x \bullet F(x,y) \\ Q(x,y) \end{pmatrix} = 0. \tag{3.3}
$$

where one starting point x^0 is took in the **set of feasible points** of MNCP, following Def. 3.1.3, this set is defined by

$$
\Omega := \{(x,y) \in \mathbb{R}^n \times \mathbb{R}^m \,:\, x \geq 0,\ F(x,y) \geq 0\}.
$$

and the interior of Ω is denoted as Ω^0.

Given an initial point inside the domain Ω, $(x^0, y^0) \in \Omega$, and then is applied the

Newton's method to (3.3), results in the iteration " k "

$$\nabla S(x^k, y^k) d_N^k = -S(x^k, y^k). \tag{3.4}$$

where

$$\nabla S(x^k, y^k) = \begin{pmatrix} \operatorname{diag}(F(x^k, y^k)) + \operatorname{diag}(x^k)\nabla_x F(x^k, y^k) & \operatorname{diag}(x^k)\nabla_y F(x^k, y^k) \\ \nabla_x Q(x^k, y^k) & \nabla_y Q(x^k, y^k) \end{pmatrix}, \tag{3.5}$$

for all $(x^k, y^k) \in \Omega$, and $\operatorname{diag}(x^k) \in \mathbb{R}^{n\times n}$ is a diagonal matrix such that $(\operatorname{diag}(x^k))_{ii} \equiv (x^k)_i$.

Notice that for System 3.4 has solution must be to exists the inverse matrix of $\nabla S(x, y)$ and we want to obtain that $(x^k, y^k) \in \Omega$ for all iteration " k ". On the other hand, all row $i = 1, \ldots, n$ of (3.5) verify that

$$[\nabla S(x^k, y^k)]_i = F_i(x^k, y^k)e_i + x_i^k \nabla F_i(x^k, y^k) \tag{3.6}$$

where e_i is the "i" row vector of canonical base of $\mathbb{R}^n$, and $\nabla F_i(x^k, y^k)$ is a row vector.

Notice that (x^{k+1}, y^{k+1}) corresponds to a search direction d_N^k of System 3.4, that is, $(x^{k+1}, y^{k+1}) = (x^k, y^k) + d_N^k$. Suppose that (x^k, y^k) is not solution of 3.1, then there exists $j \in \{1, \ldots, n\}$ such that $x_j^k F_j(x^k, y^k) \neq 0$, then the System 3.4 has not null solution and the solution is unique. Now, for each $i \in \{1, \ldots, n\}$ such that $x_i^k F_i(x^k, y^k) = 0$, from (3.4) and (3.6) obtain

$$(F_i(x^k, y^k)e_i + x_i^k \nabla F_i(x^k, y^k))d_N^k = -x_i^k F_i(x^k, y^k), \tag{3.7}$$

Since that demand that $\nabla S(x, y)$ is not singular, we have two cases

a. If $x_i^k > 0$ and $F_i(x^k, y^k) = 0$ imply $\nabla F_i(x^k, y^k)d_N^k = 0$. Thus d_N^k is tangent to restriction $F_i(x, y) \geq 0$.

b. If $x_i^k = 0$ and $F_i(x^k, y^k) > 0$ imply $d_{N,i}^k = 0$. Thus d_N^k is tangent to restriction $x_i^k \geq 0$.

Both of cases is saw that the direction d_N^k is not feasible. One geometric interpretation is similar to FDA–NCP, which the direction d_N^k is not necessarily feasible in general, see Figure 2.1.

The next result guarantees when a vector $d \in \mathbb{R}^{n+m}$ is a feasible direction to Ω.

Proposition 3.1.1. *Let $d \in \mathbb{R}^{n+m}$ and $(x, y) \in \Omega$. If d satisfies the conditions*

a. $d_i > 0$ for all $i \in \{1, \ldots, n\}$ such that $x_i = 0$, and

b. $d^T \nabla F_i(x, y) > 0$ for all $i \in \{1, \ldots, n\}$ such that $F_i(x, y) = 0$,

then d is a feasible direction of the MNCP at (x, y).

Proof. Since $(x, y) \in \Omega$ then $x \geq 0$ and $F(x, y) \geq 0$. We want to prove that there exists $\hat{\alpha} > 0$ such that $(x, y) + \alpha d \in \Omega$ for all $\alpha \in (0, \hat{\alpha}]$.
By Taylor's theorem for each $F_i \, (i = 1, \ldots, n)$ obtain

$$F_i((x, y)+\alpha d) = F_i(x, y)+\alpha d^T \nabla F_i(x, y)+o(\alpha) = F_i(x, y)+\alpha \left(d^T \nabla F_i(x, y) + \frac{|o(\alpha)|}{\alpha} \right), \tag{3.8}$$

such that

$$\lim_{\alpha \to 0} \frac{|o(\alpha)|}{\alpha} = 0. \tag{3.9}$$

From (3.9) obtain that there exists $\hat{\alpha}_i > 0$ such that

$$0 < d^T \nabla F_i(x, y) + \frac{|o(\alpha)|}{\alpha} < 2 d^T \nabla F_i(x, y) \quad \text{for all} \quad \alpha \in (0, \hat{\alpha}_i]. \tag{3.10}$$

Considering (3.8), $\hat{\alpha} = \min\{\hat{\alpha}_i\}$ and (b) is guaranted that $F((x, y) + \alpha d) \geq 0$. Since $x_i + \alpha d \to x_i$ when $\alpha \to 0$ and (a), without loss generality , we can consider $\hat{\alpha}$ such that $x_i + \alpha d_i \geq 0$ and $F_i((x, y) + \alpha d) \geq 0$ for all $\alpha \in (0, \hat{\alpha}]$ and $i = 1, \ldots, n$. □

Proposition 3.1.1 gives a condition such that a direction d can be a feasible direction in Ω. In order to obtain this direction, we consider the direction $d_R^k \in \mathbb{R}^{n+m}$ as solution of next system

$$\nabla S(x^k, y^k) d_R^k = \rho^k E, \tag{3.11}$$

where ρ^k is a positive parameter and $E \in \mathbb{R}^{n+m}$ is going to be a adequate non null vector such that E guarantees that d_R^k satisfies Proposition 3.1.1. The direction d_R^k is called **restoration direction**.

Again, if $(x^k, y^k) \in \Omega$ is not solution of 3.1, then there exists $j \in \{1, \ldots, n\}$ such that $x_j^k F_j(x^k, y^k) \neq 0$ and since $E \neq 0$ then the System 3.11 has d_R^k as non null and unique solution. From (3.11) and (3.6), for each row $i \in \{1, \ldots, n\}$ such that $x_i^k F_i(x^k, y^k) = 0$ holds

$$(F_i(x^k, y^k)e_i + x_i^k \nabla F_i(x^k, y^k))d_R^k = \rho^k E_i, \tag{3.12}$$

Since that $\nabla S(x, y)$ is not singular, we analyze from (3.12) the unique two cases

a. If $x_i^k > 0$ and $F_i(x^k, y^k) = 0$ imply $\nabla F_i(x^k, y^k)d_R^k = \rho^k \dfrac{E_i}{x_i^k}$.

b. If $x_i^k = 0$ and $F_i(x^k, y^k) > 0$ imply $d_{R,i}^k = \dfrac{\rho^k E_i}{F_i(x^k, y^k)}$.

In order to guarantee d_k^R be a feasible direction, it has to satisfies $(a) - (b)$. If we choose vector E as an positive vector, then we get that.

In the end, we define the next vector:

$$d^k = d_N^k + d_R^k \tag{3.13}$$

Thus, the problem found by Newton's method, which does not generate feasible direction is circumvented by d^k defined by (3.13). We can observe that d^k is solution of the perturbed Newton's iteration as follows

$$\nabla S(x^k, y^k)d^k = \begin{pmatrix} -x^k \bullet F(x^k, y^k) \\ -Q(x^k, y^k) \end{pmatrix} + \rho^k E, \tag{3.14}$$

On the other hand, following a similar idea to FDA–NCP is defined one **potential function** as follows

$$f(x, y) \equiv \phi(x, y) + \|Q(x, y)\|^2, \tag{3.15}$$

and we want to generate with FDA–MNCP a sequence of points such that the potential function in (3.15) decreases at each iteration in the direction d^k defined by (3.13), where $\phi(x, y) = x^T F(x, y)$. For that, we use the next result for that a direction d be a descent direction.

Proposition 3.1.2. *If $f : \mathbb{R}^n \to \mathbb{R}$ is a differentiable function at x and $d \in \mathbb{R}^n$ such that $\nabla f(x)\, d^T < 0$, then d is a descent direction of function f.*

Proof. By Taylor's theorem, we have

$$f(x + \alpha d) = f(x) + \alpha \nabla f(x)\, d^T + o(\alpha),$$

where $o(\alpha)$ satisfies (3.9). From (3.9), there exists $\hat{\alpha} > 0$ such that

$$\frac{|o(\alpha)|}{\alpha} < |d^T \nabla f(x)|.$$

This, together with our assumption that $d^T \nabla f(x) < 0$, implies that for all $\alpha \in (0, \hat{\alpha}]$ we must have

$$f(x + \alpha d) - f(x) < 0.$$

Hence, d is a descent direction.

□

So, from (3.15) yields

$$\nabla f(x^k, y^k) = (R_1^T \;\; 2Q(x^k, y^k))^T \nabla S(x^k, y^k).$$

where $R_1 = [1, ..., 1]^T \in \mathbb{R}^n$. Multiplying the last equation by d^k and using (3.14) yields:

$$\nabla f(x^k, y^k)\, d^k = (R_1^T \;\; 2Q^T(x^k, y^k)) \left[\rho^k \begin{pmatrix} E_1 \\ E_0 \end{pmatrix} - \begin{pmatrix} x^k \bullet F(x^k, y^k) \\ Q(x^k, y^k) \end{pmatrix} \right], \quad (3.16)$$

where $E = \begin{pmatrix} E_1 \\ E_0 \end{pmatrix}$ such that $E_1 \in \mathbb{R}^n_+$ and $E_0 \in \mathbb{R}^m$. After some algebraic manipulations (3.16) results in

$$\nabla f(x^k, y^k)\, d^k = -2f(x^k, y^k) + \phi(x^k, y^k) + \rho^k \sum_{i=1}^{n} E_i + 2\rho^k \sum_{j=1}^{m} Q_j(x^k, y^k) E_{n+j}. \quad (3.17)$$

In order to obtain d^k as an descent direction, we choose

$$E_0 = (E_{n+j})_{j=1}^m = [0, ..., 0]^T \in \mathbb{R}^m. \tag{3.18}$$

Thus we obtain

$$\nabla f(x^k, y^k)\, d^k = -2f(x^k, y^k) + \phi(x^k, y^k) + \rho^k \sum_{i=1}^{n} E_i. \tag{3.19}$$

Now, we suppose that

$$\rho^k \sum_{i=1}^{n} E_i = \rho^0 \phi^\beta(x^k, y^k), \quad (\rho^0 > 0). \tag{3.20}$$

Substituing in (3.19)

$$\nabla f(x^k, y^k)\, d^k = -2\left[f(x^k, y^k) - \frac{1 + \rho_0 \phi^{\beta-1}(x^k, y^k)}{2}\phi(x^k, y^k)\right]. \tag{3.21}$$

In order to apply Proposition 3.1.2 to function f, we have to do

$$f(x^k, y^k) - \frac{1 + \rho_0 \phi^{\beta-1}(x^k, y^k)}{2} > 0. \tag{3.22}$$

The definition of f and (3.22) imply

$$\rho_0 \phi^{\beta-1}(x^k, y^k) < 1. \tag{3.23}$$

Under this last condition, we can conclude from (3.21) that d^k is a descent direction to function f. For simplicity, in (3.20) we choose

$$E_1 = (E_i)_{i=1}^n = [1, ..., 1]^T \in \mathbb{R}^n. \tag{3.24}$$

This election gives a simple form to calculate ρ^k as follows

$$\rho^k = \frac{\rho_0 \phi^\beta(x^k, y^k)}{n} \in]0, 1[. \tag{3.25}$$

This work seeks the solution of MNCP in the following set

$$\Omega_c := \{(x, y) \in \Omega^\circ \ : \ f(x, y) \leq c\}. \tag{3.26}$$

for some fixed real number $c > 0$. From (3.23) and (3.26), we can consider the parameters

$$\alpha \in]0, 1[, \quad \beta \in]1, 2]; \tag{3.27}$$

$$\rho_0 = \alpha \min\{1, 1/(c^{\beta-1})\}, \tag{3.28}$$

On the other hand, one common difficulty concerning the interior point methods is checking if the chosen initial point is feasible. FDA-MNCP circumvents this difficulty by working inside the set Ω_c given in (3.26), whose definition is simple to verify.

Then, a new iteration is obtained by performing an inexact line search procedure that looks for a new feasible point with a sufficient reduction of the potential function $f(x, y)$. We employ an extension of Armijo's line search that deals with inequality constraints proposed in [22]. Line search procedures based on Wolfe's or Goldstein's inexact line search criteria can also be employed [60, 21].

In Section 3.3.2 are given some assumptions about F, Q, Ω_c such that the sequence generated by FDA–MNCP converges to a solution of MNCP.

3.2 Description of the algorithm FDA–MNCP

The parameters described in (3.23)–(3.28) are used in the Algorithm 2.

This algorithm is a perturbation to Newton's iterations. Below we prove that under standard assumptions the rate of convergence of the presented method is superlinear. Thus, a smaller ρ^k will result in faster convergence. That is why, when near a solution, the algorithm considers $\rho^k = O(\phi^\beta(x^k, y^k))$. The presented algorithm is easy to implement and requires computational resources similar to that of Newton's method for a system of nonlinear equations.

As far as we know, there is no other feasible direction methods addressing MNCP. However, in the literature there are methods addressing MNCP using variations of Newton's method [11, 19, 61] and for Linear Complementarity Problems by interior point techniques [11]. There are important advantages in using feasible point techniques. From mathematical point of view, in some problems [25] the function F is not defined outside the feasible region, turning tricky application of other techniques.

Algorithm 2: FDA–MNCP

Parameters: $c > 0$, $\alpha, \eta, \nu \in (0,1)$, $\beta \in]1,2]$ y $\rho_0 < \alpha \min\{1, 1/(c^{\beta-1})\}$.

$$\epsilon > 0 \ , \ E_0 = [0, ..., 0]^T \in \mathbb{R}^m, E_1 = [1, ..., 1]^T \in \mathbb{R}^n.$$

Data: $(x^0, y^0) \in \text{int}(\Omega)$ tal que $f(x^0, y^0) < c$. Tolerancia

Result: (x^k, y^k) as a solution aproximate of MNCP.

initialization;

$k \leftarrow 0$;

while $|f(x^k, y^k)| > \textit{Tolerancia}$ **do**

Calcule the search direction $d^k = (d_x^k, d_y^k)^T$ resolving the system

$$\nabla S(x^k, y^k) d^k = \begin{pmatrix} -x^k \bullet F(x^k, y^k) + \rho^k E_1 \\ -Q(x^k, y^k) \end{pmatrix},$$

where $\rho^k = \rho_0 \frac{\phi^\beta(x^k, y^k)}{n}$.

Armijo's linear search. Choose t^k as the first number of sequence $1, \nu, \nu^2, \nu^3, ...$ such that

$$x^k + t^k d_x^k \geq 0, \tag{3.29}$$

$$F(x^k + t^k d_x^k, y^k + t^k d_y^k) \geq 0, \tag{3.30}$$

$$f(x^k + t^k d_x^k, y^k + t^k d_y^k) \leq f(x^k, y^k) + t^k \eta \nabla f(x^k, y^k)^t d^k. \tag{3.31}$$

Update: $(x^{k+1}, y^{k+1}) := (x^k + t^k d_x^k, y^k + t^k d_y^k)$.

$k \leftarrow k + 1$

end while

Output: (x^k, y^k) is a aproximate solution of MNCP.

From the perspective of applications, the intermediate steps in the algorithm are in agreement with the physics of the problem. Moreover, the stop criteria are always approximated. When the iterates approximate the solution from the outside the feasible region, there is a possibility to stop at an unfeasible point. In this case it may be possible to recover the feasibility at the price of increasing an error of the complementarity value.

3.3 Theoretical results

This section provides theoretical background for the choice of the direction d^k of System (3.14) as well as global and asymptotic convergence of FDA-MNCP. First steps in this direction were made by Mazorche [25].

3.3.1 The search direction

Proposition 3.3.1 (Feasible direction)**.** *Consider a point $(x^k, y^k) \in \Omega_c$ and the direction d^k obtained as a solution of System* (3.14)*. Then d^k is a feasible direction in Ω whenever*

$$x^k \bullet F(x^k, y^k) \neq 0.$$

Proof. Since $(x^k, y^k) \in \Omega_c$ and $x^k \bullet F(x^k, y^k) \neq 0$ it follows that ρ_0 and ρ^k given in (3.25) are well defined. From (3.14), for each row $i = 1, 2, \ldots, n$, follows

$$[F_i(x^k, y^k)e_i + x_i^k \nabla F_i(x^k, y^k)]d^k = -x_i^k F_i(x^k, y^k) + \rho^k,$$

where e_i is the vector of the canonical base of $\mathbb{R}^n$. The two following cases are important: If $x_i^k = 0$ and $F_i(x^k, y^k) > 0$, then $d_i^k = \rho^k / F_i(x^k, y^k) > 0$; If $x_i > 0$ and $F_i(x^k, y^k) = 0$, then $\nabla F_i(x^k, y^k)d^k = \rho^k / x_i > 0$. From Proposition 3.1.1 follows that d^k is a feasible direction at $(x^k, y^k) \in \Omega$ □

Proposition 3.3.2 (Descent direction)**.** *The search direction d^k obtained as a solution of System* (3.14) *is a descent direction for $f(x^k, y^k)$ at any $(x^k, y^k) \in \Omega_c$ whenever $x^k \bullet F(x^k, y^k) \neq 0$ is true and the conditions established in* (3.23)–(3.28) *are valid.*

Proof. Since $x^k \bullet F(x^k, y^k) \neq 0$ and $(x^k, y^k) \in \Omega_c$ then $c \neq 0$. From (3.15) it follows

$$\nabla f(x^k, y^k) = (E_1^T \;\; 2Q(x^k, y^k))^T \nabla S(x^k, y^k).$$

Multiplying the last equation by d^k and using (3.14) and (3.25) after some algebraic manipulations results in

$$\nabla f(x^k, y^k)\, d^k = -2\left[f(x^k, y^k) - \frac{1 + \rho_0 \phi^{\beta-1}(x^k, y^k)}{2}\phi(x^k, y^k)\right] < 0. \tag{3.32}$$

We conclude that d^k is a descent direction. □

3.3.2 Global convergence of FDA-MNCP

In order to prove global convergence the following assumptions are necessary:

Assumption 3.3.1. *The set Ω_c given by* (3.26) *is a compact set and it has an nonempty interior Ω_c^0. Each $(x, y) \in \Omega_c^0$ satisfies $x > 0$ and $F(x, y) > 0$.*

Assumption 3.3.2. *Functions $F(x, y)$, $Q(x, y)$ are continuously differentiable, $\nabla F(x, y)$ and $\nabla Q(x, y)$ satisfy Lipschitz conditions*

$$\|\nabla F(x_2, y_2) - \nabla F(x_1, y_1)\| \leq \gamma \|(x_2, y_2) - (x_1, y_1)\|, \quad \textit{and,}$$

$$\|\nabla Q(x_2, y_2) - \nabla Q(x_1, y_1)\| \leq L \|(x_2, y_2) - (x_1, y_1)\|,$$

for any $(x_1, y_1), (x_2, y_2) \in \Omega_c$, where γ and L are real positive numbers.

Assumption 3.3.3. *The matrix $\nabla S(x, y)$ given in* (3.5) *is invertible in Ω_c.*

Assumption 3.3.4. *There is a real constant $\sigma > 0$, such that the subset*

$$\Omega^* := \{(x, y) \in \Omega_c : \ \sigma \|Q(x, y)\| \leq \phi(x, y)\}$$

is nonempty.

Assumptions 3.3.1–3.3.4 imply that x and $F(x, y)$ are nonzero simultaneously for $(x, y) \in \Omega_c$, which means that the linear system (3.14) always possesses a solution. Since $\nabla F(x^k, y^k)$ and $\nabla Q(x^k, y^k)$ are continuous, the matrix in Assumption 3.3.3 possesses a continuous inverse in Ω_c. Thus, there exists a scalar $\kappa > 0$, such that $\|\nabla S(x^k, y^k)^{-1}\| \leq \kappa$ for any $(x^k, y^k) \in \Omega_c$. The following results prove that the sequence of search direction $\{d^k\}$ of the present algorithm is bounded and constitutes a uniformly feasible directions field for $\beta \in (1, 2]$ in Ω_c, i.e., there exists $\bar{\xi} > 0$ such that for any $(x^k, y^k) \in \Omega_c$ it follows that $(x^k, y^k) + td^k \in \Omega_c$ for all $t \in [0, \bar{\xi}]$.

Lemma 3.3.1. *Under Assumptions 3.3.3–3.3.4, for any $(x^k, y^k) \in \Omega^*$, there is a constant $\bar{\kappa}$ such that the search direction d^k satisfies $\|d^k\| \leq \bar{\kappa}\phi(x^k, y^k) \leq \bar{\kappa}c$.*

Proof. Let $E = (E_1 \ \ E_0)^T \in \mathbb{R}^n \times \mathbb{R}^m$, where E_1, E_0 are given in (3.18) and (3.24). It follows that:

$$\|\rho^k E - S(x^k, y^k)\|^2 \ = \ \|x^k \bullet F(x^k, y^k)\|^2 - 2\rho^k \phi(x^k, y^k) + n(\rho^k)^2 + \|Q(x^k, y^k)\|^2. \quad (3.33)$$

Similarly to what was done by Herskovits and Mazorche in [24], it is possible to find a bound to the left side of Eq. (3.33). Define

$$T := \|x^k \bullet F(x^k, y^k)\|^2 - 2\rho^k \phi(x^k, y^k) + n(\rho^k)^2$$

and observe that from the definition of ϕ in (3.15) it follows that $\|x^k \bullet F(x^k, y^k)\|^2 \leq \phi^2(x^k, y^k)$. Using it results in

$$T \leq (\phi(x^k, y^k) - \rho^k)^2 + (n-1)(\rho^k)^2.$$

Substituting ρ^k from (3.25) we obtain:

$$T \leq \left[\frac{(n - \rho_0 \phi^{\beta-1}(x^k, y^k))^2 + (n-1)(\rho_0 \phi^{\beta-1}(x^k, y^k))^2}{n^2}\right] \phi^2(x^k, y^k). \tag{3.34}$$

The third condition in (3.25) results in $n - 1 < n - \rho_0 \phi^{\beta-1}(x^k, y^k) < n$. Substituting it in (3.34) yields

$$T \leq \left(n - \rho_0 \phi^{\beta-1}(x^k, y^k)\right) \phi^2(x^k, y^k)/n < \phi^2(x^k, y^k).$$

Using (3.33) and Assumption 3.3.4 yields

$$\|\rho^k E - S(x^k, y^k)\|^2 \leq \phi^2(x^k, y^k) + \|Q(x^k, y^k)\| \leq (1 + 1/\sigma^2)\phi(x^k, y^k)^2.$$

Considering (3.14) we obtain

$$\|d^k\| \leq \bar{\kappa} \|\rho^k E - S(x^k, y^k)\|,$$

where $\bar{\kappa} = \kappa\sqrt{1 + 1/\sigma^2}$. As consequence $\|d^k\| \leq \bar{\kappa} c$. □

Lemma 3.3.2. *Consider the sequence of search directions $\{d^k\}$ given by FDA–MNCP. Under Assumptions 3.3.2–3.3.3 there exists $\Theta > 0$, such that for all $(x^k, y^k) \in \Omega_c$ holds $(x^{k+1}, y^{k+1}) = (x^k, y^k) + \tau d^k \in \Omega$ for all $\tau \in [0, \Theta]$.*

Proof. By Assumption 3.3.2, $\nabla S(x, y)$ is Lipschitz with some constant γ.
Let $(x^k, y^k) \in \Omega_c$, Proposition 3.3.1 implies that there exists $\theta > 0$, such that $[(x^k, y^k), (x^k, y^k) + \tau d^k] \subset \Omega$ for $\tau \in [0, \theta]$. From the Mean Value Theorem, after some calculations it follows that for all $\tau \in [0, \theta]$, $\tau \leq \min\{1, \rho^k/\gamma\|d^k\|^2\}$:

$$S_i((x^k, y^k) + \tau d^k) \geq 0 \quad \text{for all } i = 1, 2, ..., n. \tag{3.35}$$

Notice that

$$S_i((x^k, y^k) + \tau d^k) = x^{k+1} F_i(x^{k+1}, y^{k+1})$$

yielding $x^{k+1} \geq 0$ and $F_i(x^{k+1}, y^{k+1}) \geq 0$ (see Lemma 4.1.6 in [25] for details). It follows that $(x^k, y^k) + \tau d^k \in \Omega$. Considering Lemma 3.3.1 and ρ^k defined in (3.25), Eq. (3.35) holds for $\tau \leq \min\left\{1, \rho_0 \phi(x^k, y^k)^{\beta-2}/(\gamma n \bar{\kappa}^2)\right\}$. Since $\beta \in]1, 2]$, the present lemma is valid for $\Theta = \min\left\{1, \rho_0 c^{\beta-2}/\gamma n \bar{\kappa}^2\right\}$. □

Lemma 3.3.3. *Under Assumptions 3.3.3–3.3.4, there exists $\zeta > 0$ such that, for $(x^k, y^k) \in \Omega_c$, the Armijo's line search given by (3.31) is satisfied for any $t^k \in [0, \zeta]$.*

Proof. Let $t^k \in]0, \Theta]$, where Θ was obtained in the previous lemma. Applying the Mean Value Theorem for $i = 1, 2, ..., n$ results in

$$S_i(x^{k+1}, y^{k+1}) \leq S_i(x^k, y^k) + t^k \nabla S_i(x^k, y^k)\, d^k + (t^k)^2 \gamma \|d^k\|^2.$$

Adding the previous n inequalities and substituting the value of $\nabla S_i(x^k, y^k)\, d^k$ yields

$$\phi(x^{k+1}, y^{k+1}) \leq (1 - t^k)\phi(x^k, y^k) + t^k n \rho^k + n t^{k^2} \gamma \|d^k\|^2. \tag{3.36}$$

Similarly, applying the Mean Value Theorem for Q_i^2 yields

$$\|Q(x^{k+1}, y^{k+1})\|^2 \leq (1 - t^k)\|Q(x^k, y^k)\|^2 + m(t^k)^2 \gamma \|d^k\|^2. \tag{3.37}$$

Adding (3.36) and (3.37) the limitation for f is obtained

$$f(x^{k+1}, y^{k+1}) \leq (1 - t^k) f(x^k, y^k) + t^k [\, n\rho^k + (n + m) t^k \gamma \|d^k\|^2 \,].$$

Definition of ρ^k in (3.25) and Assumption 3.3.1 imply $1/f(x^k, y^k) \leq 1/\phi(x^k, y^k)$, yielding

$$f(x^{k+1}, y^{k+1}) \leq \left[1 - \left(1 - \rho_0 \phi^{\beta-1}(x^k, y^k) - \frac{(n + m)\gamma \|d^k\|^2 t^k}{\phi(x^k, y^k)}\right) t^k\right] f(x^k, y^k).$$

In order for Armijo's line search (3.31) to be satisfied, it is sufficient that

$$(1 - \rho_0 \phi^{\beta-1}(x^k, y^k)) - (n + m)\gamma \|d^k\|^2 t^k / \phi(x^k, y^k) \geq \eta(1 - \rho_0 \phi^{\beta-1}(x^k, y^k)).$$

As in the previous lemma, it follows

$$t^k \leq (1 - \eta)(1 - \rho_0 \phi^{\beta-1}(x^k, y^k))\phi(x^k, y^k)/((n + m)\gamma \|d^k\|^2).$$

Considering Θ from Lemma 3.3.2, from Lemma 3.3.1 the result follows for

$$\zeta = \min\left\{\frac{(1-\eta)(1-\rho_0 c^{\beta-1})}{(n+m)\gamma\bar{\kappa}^2 c^3}, \Theta\right\}.$$

□

Lemma 3.3.4. *Under Assumptions 3.3.3 and 3.3.4 there exists $\bar{\xi} > 0$ such that, for $(x^k, y^k) \in \Omega^*$, the point $(x^{k+1}, y^{k+1}) = (x^k, y^k) + t^k d^k$ belongs to set Ω^* for any $t^k \in [0, \bar{\xi}]$.*

Proof. By Lemmas 3.3.2 and 3.3.3 there exists $\zeta > 0$, such that $(x^{k+1}, y^{k+1}) = (x^k, y^k) + t^k d^k \in \Omega_c$ for all $(x^k, y^k) \in \Omega^*$, d^k is generated by FDA–MNCP and $t^k \in [0, \zeta]$. We are going to prove that $(x^{k+1}, y^{k+1}) \in \Omega^*$. Similarly to Lemma 3.3.3 applying the Mean Value Theorem to S_i $(i = 1, 2, ..., n)$ results in

$$\phi(x^{k+1}, y^{k+1}) \geq (1 - t^k)\phi(x^k, y^k) + nt^k\rho^k - n(t^k)^2\gamma\|d^k\|^2. \tag{3.38}$$

Using the Second Fundamental Theorem of Calculus for each Q_i $(i = 1, ..., m)$:

$$Q(x^{k+1}, y^{k+1}) = Q(x^k, y^k) + t^k\left[\int_0^1 \nabla Q((x^k, y^k) + \theta t^k d^k)\, d^k\, d\theta\right]. \tag{3.39}$$

Substituting $\nabla Q(x^k, y^k)d^k = -Q(x^k, y^k)$ from (3.14) into (3.39), calculating l_2 norm, multiplying by $-\sigma$ and adding it to (3.38) yields

$$\begin{aligned}&\phi(x^{k+1}, y^{k+1}) - \sigma\|Q(x^{k+1}, y^{k+1})\| \geq \\ &\quad (1 - t^k)[\phi(x^k, y^k) - \sigma\,\|Q(x^k, y^k)\|] + t^k[n\rho^k - (n\gamma + \sigma L)\|d^k\|^2 t^k].\end{aligned}$$

In order to guarantee that the right side is positive it is sufficient that

$$n\rho^k - (n\gamma + \sigma L)\|d^k\|^2 t^k > 0.$$

Using the definition of ρ^k we obtain that

$$t^k \leq \delta\left(\rho^k/(\gamma\,\|d^k\|^2)\right),$$

where $\delta = n\gamma/(n\gamma + \sigma L) \in]0, 1]$.
It follows that $(x^{k+1}, y^{k+1}) \in \Omega^*$, for all $t^k \in]0, \bar{\xi})$ and $\bar{\xi} = \min\left\{\delta\rho_0 c^{\beta-2}/(\gamma\,\bar{\kappa}^2 n), \zeta\right\}$.

□

As a consequence of the three previous lemmas, the sequence $\{d^k\}$ generated by FDA–MNCP is a uniformly feasible directions field in Ω_c. Moreover, the number of steps required by Armijo's line search described in Step 2 of the algorithm is finite and bounded from above. The following theorem addresses the global convergence of the presented algorithm.

Theorem 3.3.1. *Under Assumptions 3.3.1–3.3.4, given the initial point $(x^0, y^0) \in \Omega^*$, there exists a subsequence of $\{(x^k, y^k)\}$ generated by FDA–MNCP converging to (x^*, y^*), a solution of MNCP given by Def. 3.1.3.*

Proof. From Lemmas 3.3.1–3.3.3 it follows that $(x^k, y^k) \in \Omega_c$. This, jointly with Assumption 3.3.1, implies that there exists a subsequence $\{(x^{k_n}, y^{k_n})\} \in \Omega_c$ converging to $(x^*, y^*) \in \Omega_c$. Using that f is a continuous function, Proposition 3.3.2 implies that $f(x^k, y^k)$ is a decreasing sequence converging to its infimum $f(x^*, y^*)$. If $f(x^*, y^*) \neq 0$, from the definition of f results that $\phi(x^*, y^*) \neq 0$ and the set of indexes $J := \{j \in [1, n] \,:\, x_j F_j(x^*, y^*) \neq 0\}$ is nonempty. On the other hand, $\|d^k\| \downarrow 0$ as t^k is bounded from below. From System (3.14) it follows that

$$d^k = \nabla^{-1} S(x^k, y^k)[-S(x^k, y^k) + \rho^k E].$$

Thus, $-x_i^* F_i(x^*, y^*) + \rho^0 \phi^\beta(x^*, y^*)/n = 0$, for each row $i = 1, \ldots, n$. Adding these equations it follows that $\rho^0 \phi^{\beta-1}(x^*, y^*) = 1$, contradicting the third condition in (3.25). Thus, (x^*, y^*) is the solution of MNCP. □

3.3.3 Asymptotic convergence

The present algorithm is a perturbation of Newton's iteration and it is natural to expect a rate of convergence close to quadratic for smaller values of ρ^k. Unfortunately, a unitary step-length can not be always ensured. The present approach possesses asymptotic convergence as formulated next result.

Theorem 3.3.2. *Consider the sequence $\{(x^k, y^k)\}$ generated by FDA-MNCP that converges to a solution (x^*, y^*) of MNCP given by Def. 3.1.3. Then: (i) Taking $\beta \in]1, 2[$ and $t^k = 1$ for k large enough, the rate of convergence of the present algorithm is at least super-linear; (ii) If $t^k = 1$ for large k and $\beta = 2$, then the rate of convergence is quadratic.*

Proof. Considering Θ from Lemma 3.3.2, $\bar{\xi}$ from Lemma 3.3.4 and $t^k \in]0, min\{\Theta, \bar{\xi}\}]$, it follows that

$$\begin{aligned} \|(x^{k+1}, y^{k+1}) - (x^*, y^*)\| &\leq (1 - t^k)\|(x^k, y^k) - (x^*, y^*)\| + \\ \kappa\rho_0\phi^\beta(x^k, y^k)/\sqrt{n} &+ O(\|(x^k, y^k) - (x^*, y^*)\|^2). \end{aligned} \tag{3.40}$$

From the Mean Value Theorem and the Lipschitz condition it follows that

$$\phi^\beta(x_1, y_1) \leq \phi^\beta(x_2, y_2) + \beta\phi^{\beta-1}(\bar{x}, \bar{y})\sqrt{n}\, O(\|(x_1, y_1) - (x_2, y_2)\|),$$

where $(\bar{x}, \bar{y}) = (x_2, y_2) + \epsilon((x_1, y_1) - (x_2, y_2))$ for some $\epsilon \in]0, 1[$. Taking $(x_2, y_2) = (x^*, y^*)$, for all $(x_1, y_1) = (x^k, y^k)$ sufficiently near (x^*, y^*) it is equivalent to

$$\phi^\beta(x^k, y^k) \leq \phi^{\beta-1}(\bar{x}, \bar{y})\beta\sqrt{n}\, O(\|(x^k, y^k) - (x^*, y^*)\|). \tag{3.41}$$

(i) Hypothesis $\beta \in]1, 2[$ and $t^k = 1$ for large k in (3.41) imply

$$\phi^\beta(x^k, y^k) = O(\|(x^k, y^k) - (x^*, y^*)\|).$$

By substitution in (3.40) we obtain that $\lim_{k\to\infty} \frac{\|(x^{k+1}, y^{k+1}) - (x^*, y^*)\|}{\|(x^k, y^k) - (x^*, y^*)\|} = 0$. Thus, the rate of convergence is super-linear.

(ii) The result for $\beta = 2$ is obtained in a similar way. □

3.4 Benchmark problems

To test the numerical behavior of the present algorithm, a number of problems presented in the literature are solved. The numerical implementation considers $\rho_0 = \alpha \min\{1, \phi^{\beta-1}(x^k, y^k)\}$ in order to avoid extremely large deflections far from the solution and ρ_0 is constant when $\phi(x^k, y^k)$ is small. All the simulations were performed for two cases: $\beta = 1.1$ and $\beta = 2$. All problems were solved with the same parameters: $\alpha = 0.25$, $\eta = 0.4$, $\nu = 0.8$ and the stop criteria $f(x^k, y^k) < 10^{-8}$. For each test problem, 10 different starting points were considered. The complementarity condition used is $(w,\ v)^T \bullet F(w, v, x) = 0$, where w, v have different dimensions for each test problem. The results are summarized in Table **??** for the values $\beta = 1.1$ and $\beta = 2$, where Min and Max represent the minimun and maximun numbers of

iterations. As shown in Table 3.1 and Table 3.2 for different initial points the number of iterations does not change significantly for both analyzed values of parameter β. The exception is $\beta = 1.1$ for the problem 4.10, which presented bad convergence due to strong nonlinearity presented in this example. The present algorithm converged in all tested benchmark problems showing the robustness of FDA–MNCP.

Table 3.1: Number of iterations for the benchmark problems to converge.

β \ Problem		3.4.1	3.4.2	3.4.3	3.4.4	3.4.5
1.1	Min	24	23	16	15	15
	Max	25	25	22	16	20
2	Min	22	20	14	12	13
	Max	23	23	19	13	20

Table 3.2: Number of iterations for the benchmark problems to converge.

β \ Problem		3.4.6	3.4.7	3.4.8	3.4.9a	3.4.9b	3.4.10
1.1	Min	16	13	13	11	11	104542
	Max	18	17	14	13	14	471302
2	Min	14	13	10	13	13	21
	Max	21	18	17	16	17	40

Problem 3.4.1 (Example 3.5 [16])**.** *This problem is proposed as NCP and solved as MNCP using* (3.2) *with* $l_i = 0, u_i = M = 10^5$, $i = 1, 2$. *This problem consists in searching for* $(w, v) \in \mathbb{R}^2_+ \times \mathbb{R}^2+$ *and* $x \in \mathbb{R}^2$ *such that*

$$F(w, v, x) = \begin{pmatrix} x_1 \\ x_2 \\ M - x_1 \\ M - x_2 \end{pmatrix}, Q(w, v, x) = \begin{pmatrix} (x_1 - 1)^2 \\ x_1 + x_2 - 1 \end{pmatrix} + v - w.$$

The exact solution of this problem is $(1, 0)$.

Problem 3.4.2 (Example 6.1 [16])**.** *This problem is proposed as NCP. In order to solve this problem as MNCP we use* (3.2) *with* $l_i = 0$, $u_i = M = 10^5$, $i = 1, 2$. *This*

problem consists in searching for $(w, v) \in \mathbb{R}^2_+ \times \mathbb{R}^2_+$ *and* $x \in \mathbb{R}^2$*, such that*

$$F(w,v,x) = \begin{pmatrix} x_1 \\ x_2 \\ M - x_1 \\ M - x_2 \end{pmatrix}, Q(w,v,x) = \begin{pmatrix} (x_1 - 1)^2 \\ x_1 + x_2 + x_2^2 - 1 \end{pmatrix} + v - w = 0.$$

The exact solution for this problem is $(1, 0)$*.*

Problem 3.4.3 (Example 6.2 [16])**.** *This is a minimization problem. Applying KKT conditions* [59]*, this problem can be written as MNCP in the form of Def. 3.1.3. This problem consists in searching for* $w \in \mathbb{R}^2_+$*,* $x \in \mathbb{R}^2$*, such that*

$$F(w,x) = \begin{pmatrix} x_1 \\ x_2 \end{pmatrix}, Q(w,z) = \begin{pmatrix} 2x_1 + 2x_2 - w_1 \\ 2x_1 + 2x_2 - w_2 \end{pmatrix},$$

where $w = (w_1, w_2)$ *are KKT multipliers,* $x = (x_1, x_2)$ *are the primal variables.*

Problem 3.4.4 (Example 6.3 [16])**.** *This is a minimization problem. It can be written as MNCP in the form of Def. 3.1.3 using KKT conditions from* [59]*. This problem consists in searching for* $w \in \mathbb{R}_+$*,* $x \in \mathbb{R}$*, such that*

$$F(w,x) = x,\ Q(w,x) = x^3 - w.$$

The exact solution for this problem is $x = 0$*.*

Problem 3.4.5 (Example 6.5 [16])**.** *This is a minimization problem. Applying KKT conditions given in* [59]*, this problem can be written as MNCP in the form of Def. 3.1.3. This problem consists in searching for* $w \in \mathbb{R}^2_+$*,* $x \in \mathbb{R}^2$ *such that*

$$F(w,x) = \begin{pmatrix} x_1 - \dfrac{x_2^2}{2} \\ x_1 + \dfrac{x_2^2}{2} \end{pmatrix}, Q(w,x) = \begin{pmatrix} x_1 - w_1 - w_2 \\ x_2^2 + w_1 x_2 - w_2 x_2 \end{pmatrix}.$$

This problem has the exact solution $x = (0, 0)^T$ *.*

Problem 3.4.6 (Example 3.4 [17])**.** *This is a minimization problem. Applying KKT conditions given in* [59] *this problem can be written as MNCP in the form*

of Def. 3.1.3. This problem consists in searching for $w \in \mathbb{R}^3_+$, $x \in \mathbb{R}^2$, *such that*

$$F(w,x) = \begin{pmatrix} x_1 \\ x_2 \\ x_1 + x_2 \end{pmatrix}, \; Q(w,x) = \begin{pmatrix} 1 + x_1 - w_1 - w_3, \\ x_2 - w_2 - w_3 \end{pmatrix}.$$

The exact solution for this problem is $x = (0,0)^T$.

Problem 3.4.7 (Powell's badly scaled problem [62])**.** *This problem consists of a system of nonlinear equations that can be written as MNCP* [20, 58]. *It can also be written as MNCP given by Def. 3.1.3 by using* $l_i = -u_i = -M = -10^5$, $i = 1, 2$. *It is symmetric under the transformation* $x_1 \leftrightarrow x_2$ *and it possesses two solutions* $x^* = (9.106, 1.098 \times 10^{-5})^T$; $\hat{x} = (1.098 \times 10^{-5}, 9.106)^T$. *This problem consists in searching for* $(w,v) \in \mathbb{R}^2_+ \times \mathbb{R}^2_+ \in \mathbb{R}^2$, *such that*

$$F(w,v,x) = \begin{pmatrix} x_1 + M \\ x_2 + M \\ M - x_1 \\ M - x_2 \end{pmatrix}, \; Q(w,v,x) = \begin{pmatrix} 10^4\, x_1 x_2 - 1 \\ e^{-x_1} + e^{-x_2} - 1.0001 \end{pmatrix} + v - w.$$

Problem 3.4.8 (Powell's singular function [62])**.** *This problem consists of a system of nonlinear equations and it possesses a singular Jacobian on the hyperplane* $x_1 - x_4 = 0$, *thus, the Newton's method is not applicable. The only solution of this problem is* $x = (0,0,0,0)^T$ [62]. *It can also be written as MNCP given by Def. 3.1.3 by using* $l_i = -u_i = -M = -10^5$, $i = 1, 2, 3, 4$. *This problem consists in searching for* $(w,v) \in \mathbb{R}^4_+ \times \mathbb{R}^4_+$, $x \in \mathbb{R}^4$, *such that*

$$F(w,v,x) = \begin{pmatrix} x_1 + M \\ x_2 + M \\ x_3 + M \\ x_4 + M \\ M - x_1 \\ M - x_2 \\ M - x_3 \\ M - x_4 \end{pmatrix}, \; Q(w,v,x) = \begin{pmatrix} x_1 + 10x_2 \\ \sqrt{5}(x_3 - x_4) \\ (x_2 - 2x_3)^2 \\ \sqrt{10}(x_1 - x_4)^2 \end{pmatrix} + v - w.$$

Problem 3.4.9 (Walsarian equilibrium model [14]). *The Walsarian equilibrium model, presented in as MNCP in the form Def. 3.1.1* [14]*, was rewritten as a minimization problem and solved applying the infeasible interior point algorithm. Depending on the values of the constants* $b_2, b_3 > 0$ *and* $\alpha \in (0,1)$*, this problem possesses different solutions. For numerical results is used* $(\alpha, b_2, b_3) = (0.75, 1, 0.5)$ *(4.9b in Table 3.2) and* $(0.75, 1, 2)$ *(4.9a in Table 3.2) as in* [14]*. Considering* $l_i = 0, u_i = M = 10^5$, $i = 1, 2, 3, 4$*; this problem can be written as Def. 3.1.3. This problem consists in searching for* $(w, v) \in \mathbb{R}^4_+ \times \mathbb{R}^4_+$, $\bar{x} = (z, x_1, x_2, x_3)^T \in \mathbb{R}^4$*, such that*

$$F(w,v,\bar{x}) = \begin{pmatrix} z \\ \bar{x}_1 \\ \bar{x}_2 \\ \bar{x}_3 \\ M - z \\ M - \bar{x}_1 \\ M - \bar{x}_2 \\ M - \bar{x}_3 \end{pmatrix}, \; Q(w,v,\bar{x}) = \begin{pmatrix} -x_1 + x_2 + x_3 \\ z - \alpha \dfrac{(b_2 x_2 + b_3 x_3)}{x_1} \\ b_2 - z - (1-\alpha)\dfrac{(b_2 x_2 + b_3 x_3)}{x_2} \\ b_3 - z \end{pmatrix} + v - w.$$

Problem 3.4.10 (Kojima–Shindo's Problem [14, 63, 64]). *This problem was proposed as NCP and solved by using Algorithms EN and EQN* [64]*, by using quasi Newton's methods* [63] *and by using NLCP algorithm* [14]*. The exact solutions are* $\bar{x} = (\sqrt{6}/2, 0, 0, 0.5)$ *and* $\bar{x} = (1, 0, 3, 0)$*. It is possible to write it in the form of Def. 3.1.3 using* $l_i = 0, u_i = M = 10^5$, $i = 1, 2, 3, 4$*. This problem consists in searching for* $(w, v) \in \mathbb{R}^4_+ \times \mathbb{R}^4_+$, $x \in \mathbb{R}^4$*, such that*

$$F(w,v,x) = \begin{pmatrix} x_1 \\ x_2 \\ x_3 \\ x_4 \\ M - x_1 \\ M - x_2 \\ M - x_3 \\ M - x_4 \end{pmatrix}, \; Q(w,v,x) = \begin{pmatrix} 3x_1^2 + 2x_1x_2 + 2x_2^2 + x_3 + 3x_4 - 6 \\ 2x_1^2 + x_1 + x_2^2 + 10x_3 + 2x_4 - 2 \\ 3x_1^2 + x_1x_2 + 2x_2^2 + 2x_3 + 9x_4 - 9 \\ x_1^2 + 3x_2^2 + 2x_3 + 3x_4 - 3 \end{pmatrix} + v - w$$

3.5 In situ combustion models formulated as MNCP

3.5.1 Model 1

In order to write the simplest model given by System (1.5)–(1.6) as mixed nonlinear complementarity problem, is done a similar transformation to [12, 51] obtaining

$$\theta \geq 0,\ \eta \in \mathbb{R}: \quad \frac{\partial \theta}{\partial t} + u\frac{\partial(\rho\,\theta)}{\partial x} - \frac{1}{Pe_T}\frac{\partial^2 \theta}{\partial x^2} - \Phi \geq 0, \tag{3.42}$$

$$\frac{\partial \eta}{\partial t} - \Phi = 0, \tag{3.43}$$

$$\left(\frac{\partial \theta}{\partial t} + u\frac{\partial(\rho\,\theta)}{\partial x} - \frac{1}{Pe_T}\frac{\partial^2 \theta}{\partial x^2} - \Phi\right)\theta = 0, \tag{3.44}$$

We need Eq. (3.44) to be satisfied at the right end of the interval, where Eq. (1.9) may not be satisfied. This explains the choice of dimensionless variable η describing fuel depth inside the reservoir.

3.5.2 Model 2

A similar transformation done in Section 3.5.1 and following [12, 13, 51] in order to write System (1.9)-(1.11) as mixed nonlinear complementarity problem, we obtain

$$\theta \geq 0,\ Y, \eta \in \mathbb{R}: \quad \frac{\partial \theta}{\partial t} + V_T\frac{\partial \theta}{\partial x} - \frac{1}{Pe}\frac{\partial^2 \theta}{\partial x^2} - \mu_T\Phi(\theta, Y, \eta) \geq 0, \tag{3.45}$$

$$\frac{\partial Y}{\partial t} + V_Y\frac{\partial Y}{\partial x} - \lambda_Y\frac{\partial^2 Y}{\partial x^2} + \mu_Y\Phi(\theta, Y, \eta) = 0, \tag{3.46}$$

$$\frac{\partial \eta}{\partial t} + \mu_\eta\Phi(\theta, Y, \eta) = 0, \tag{3.47}$$

$$\left(\frac{\partial \theta}{\partial t} + V_T\frac{\partial \theta}{\partial x} - \lambda_T\frac{\partial^2 \theta}{\partial x^2} - \Phi\right)\theta = 0, \tag{3.48}$$

3.6 Elastic–plastic torsion problem formulated as MNCP

In order to write the System 1.13 as MNCP in the form of Definition 3.1.3 is used the weak formulation, for that the following Sobolev space is considered

$$H_0^1(\Sigma) := \{v \in H^1(\Sigma) : v = 0 \text{ on } \partial\Sigma\},$$

which is a closed vector subspace of $H^1(\Sigma)$. We seek the solution in the closed and convex subset $\hat{K}$ of $H_0^1(\Sigma)$ given by $\hat{K} := \{v \in H_0^1(\Sigma) : |v(x)| \leq 1\}$. The System (1.13) can be rewritten as a variational inequality [10],

$$\int\int_{\Sigma} \nabla u \,.\, \nabla(v-u) \geq \int\int_{\Sigma} (v-u) \quad \forall\, v \in \hat{K}, u \in \hat{K}, \tag{3.49}$$

which possesses a unique solution [65].

The Elastic–Plastic Torsion Problem in the variational formulation (3.49) is especially appropriate for a numerical solution by using the Finite Element Method (FEM) by writing it as a mixed complementarity problem, which is solved by using FDA–MNCP. The equivalence between the Elastic–Plastic Torsion Problem given by variational inequality (3.49) and same inequality substituting the set $\hat{K}$ by

$$K := \{v \in H_0^1(\Sigma) : |v(x_1, x_2)| \leq d(x_1, x_2)\}$$

was proven in [66] using $d(x_1, x_2) = \text{distance}((x_1, x_2), \partial\Sigma)$, $\forall (x_1, x_2) \in \bar{\Sigma}$.

FEM formulation used here follows [11] with a standard triangulation T_h on $\bar{\Sigma} = \Sigma \cup \partial\Sigma$. The space $H^1(\Sigma)$ is substituted by a finite dimensional discrete space V_h of piecewise polynomials v_h of degree one. Inequality (3.49) is written in a discrete form, i.e., search $u_h \in K_h$ such that

$$\int\int_{\Sigma} \nabla u_h \,.\, \nabla(v_h - u_h) \geq \int\int_{\Sigma} (v_h - u_h) \quad \forall\, v_h \in K_h. \tag{3.50}$$

Let $\{\varphi_1, ..., \varphi_n\}$ a base of V_h, where n is the number of nodes, then

$$v_h(x_1, x_2) = \sum_{j=1}^{n} v_j \varphi_j(x_1, x_2),\ z_h(x_1, x_2) = \sum_{j=1}^{n} z_j \varphi_j(x_1, x_2),$$

for each $(x_1, x_2) \in \Sigma \cup \partial\Sigma$. Replacing these expressions into (3.50), yields

$$(v - z)^T (q + Mz) \geq 0 \quad \text{for all } v \in K_h, \tag{3.51}$$

where K_h, the matrix $M = (m_{ij}) \in \mathbb{R}^{n \times n}$ and the vector $q = (q_i) \in \mathbb{R}^n$ are given by

$K_h := \{v \in \mathbb{R}^n \,:\, a_i \leq v_i \leq b_i,\ i = 1, ..., n; v_i = g_i \text{ in } \partial\Sigma \cup T_h\}$,

$$m_{ij} = \iint_{\Sigma} \left[\frac{\partial \varphi_i}{\partial x_1} \frac{\partial \varphi_j}{\partial x_1} + \frac{\partial \varphi_i}{\partial x_2} \frac{\partial \varphi_j}{\partial x_2} \right] dx_1 dx_2,$$

$$q_i = -\iint_{\Sigma} \theta \varphi(x_1, x_2) dx_1 dx_2.$$

In [11] was established that (3.51) can be written as MNCP in the form of Def. 3.1.2 setting J as the set of interior nodes and N as the number of elements of J. The problem consists in searching $w, v \in \mathbb{R}^N_+$ and $z \in \mathbb{R}^N$ such that

$$\begin{aligned} F(w, v, z) &\geq 0, \\ Q(w, v, z) &= q + Mz + v - w = 0, \end{aligned} \tag{3.52}$$

where

$$F(w, v, z) = \begin{pmatrix} z_1 - a_1 \\ \vdots \\ z_N - a_N \\ b_1 - z_1 \\ \vdots \\ b_N - z_N \end{pmatrix}, \tag{3.53}$$

The complementarity condition is given by

$$\begin{pmatrix} w \\ v \end{pmatrix} \bullet F(w, v, z) = 0. \tag{3.54}$$

The System (3.52) join to (3.54) is a MNCP, which is solved applying FDA–MNCP with FEM in Section 4.3.

Chapter 4

ANALYSIS OF NUMERICAL RESULTS

In this section are presented numerical results using FDS+FDA–NCP, FDS + FDA–MNCP and validate the solution obtained with FDS + Newton's method for in situ combustion models describes in Section 1.2.1 and Section 1.2.2. The FDS is based in Crank–Nicolson scheme described in Appendix A. The model of diffusion of oxygen and the in situ combustion models are evolutive problems, then, for numerical simultations the time is denoted by t with the time index denoted by n and the time step is $k = \Delta t$ and it is considered an homogeneous grid for the variable x with $M+1$ points, where x_0 and x_M are the boundary points of the interval of the calculation. The grid spacing is $h = x_{m+1} - x_m = 1/M$ and the grid position m corresponds to $x = m\Delta x$.

In order to solve our problems is employed the following scheme

Step 0: Start with the initial variable u_m^0, $m = 0, 1, \ldots, M$ and the first time step Δt_0.

Step 1: Obtain the discrete form as nonlinear system of equations, NCP or MNCP using FDS or FEM.

Step 2: Use Newton's method, FDA-NCP or FDA–MNCP algorithms to solve the nonlinear system of equations, NCP or MNCP respectively from step # 1.

Step 3: Use the solution from **step 2** as the variable u value at the next time step.

Repeat the algorithm from the **step 1** until reaching the final time.

The global properties do the Crank-Nicolson scheme are well known, e.g. [67]. In general, the convergence of FDS and FEM is rigorously proved only for simple equations or linear systems; see [27], however they are widely used for solving numerically reaction-diffusion equations similar to the examples addressed here [36, 42, 68, 26, 30].

In case of Elastic–Plastic Torsion problem described in Section 1.3 is presented the comparison between the exact solution and the numerical results by FDA–MNCP using FEM.

4.1 Oxygen diffusion

For numerical results starts with the equilibrium solution as initial conditions and use Neumann boundary conditions at the left and right sides of the interval $\partial c/\partial x(x_0) = 0$, and $\partial c/\partial x(x_N) = 0$. The results plotted on Figure 4.1 are very similar to those shown on the Figure 3 of [26], where semi-analytical techniques were employed.

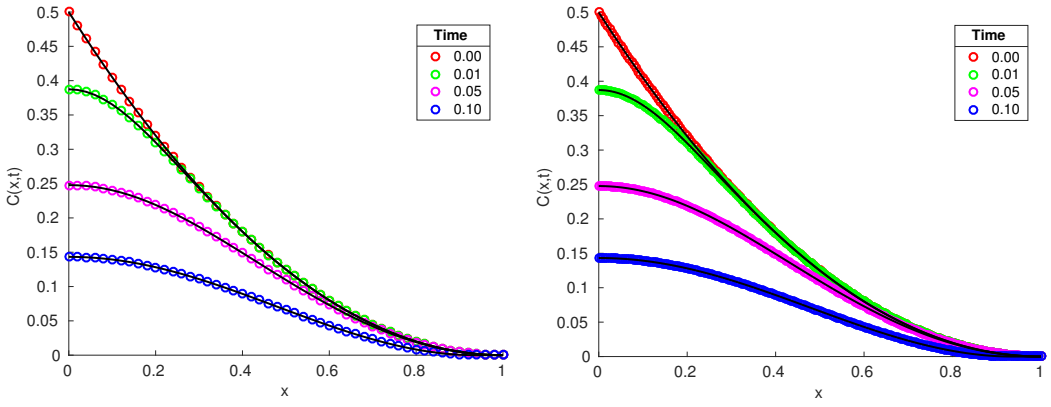

(a) $M = 51$ (b) $M = 201$

Figure 4.1: The solution obtained by using FDS + FDA-NCP (lines) is compared to one obtained with FDS+Newton's method (circles). Solutions are shown in (a) and (b) corresponding to grids with $M = 51$ and $M = 201$ points respectively. This model is solved in [37] by FEM+FDA–NCP and it shows good agreement with the literature and our results.

4.2 In situ combustion models

To compare the FDA–NCP and FDA–MNCP algorithms with the classical Newton's method, four different simulations were performed inside the interval $[0, 0.05]$ using constant time step k and space grids with 51 ($k = 10^{-5}$), 101 ($k = 5 \cdot 10^{-6}$), 201 ($k = 2.5 \cdot 10^{-6}$) and 401 ($k = 1.25 \cdot 10^{-6}$) points.

4.2.1 Model 1

For this model is considered the following dimensionless parameters values, see [36, 12]:

$$\mathrm{Pe}_T = 1406, \beta = 7.44 \cdot 10^{10}, \mathcal{E} = 93.8, \theta_0 = 3.67, \quad \text{and} \quad u = 3.76.$$

For more details of this model and its discrete formulation as NCP is showed in [38], as MNCP is showed in Appendix A.1.1 and as a nonlinear system of equations is showed in Appendix A.1.2.

Validate the numerical solutions is not possible because we have not experimental data. In these case, analytical estimative are viable, for that, is analyzed the Riemann's problem respective. This will be done in Section 4.2.1.3.

4.2.1.1 Comparison of numerical results using FDA–NCP

Its numerical solution by FDS + FDA–NCP and FDS+Newton's method were published in [12, 38]. Using FEM+FDA–NCP and FEM+Newton's method were published in [12] and all numerical solutions can be see in Figure 4.2–4.3.

4.2.1.2 Comparison of numerical results using FDA–MNCP

The comparison of numerical results obtained by FDS+FDA–MNCP and FDS + Newton's method are showed in Figure 4.4 (a), (b), (c) and (d). Over there can observed that the numerical results are almost equals. In Figure 4.5 are compared the numerical results obtained by FDS+FDA–NCP and FDS+FDA–MNCP for the same model.

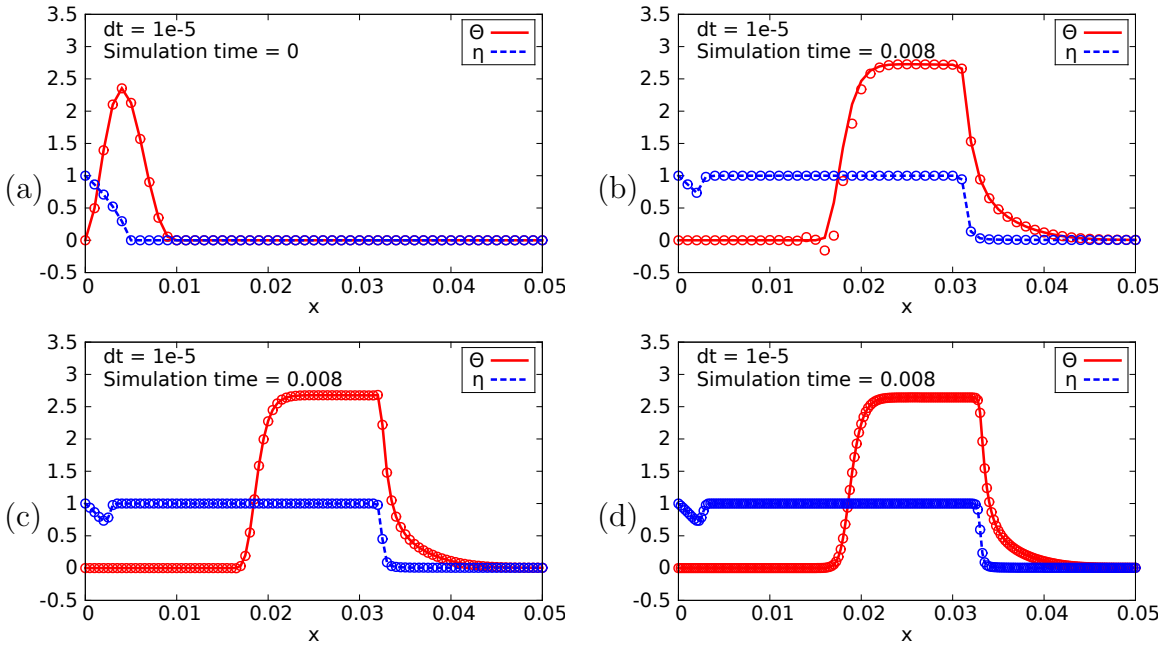

Figure 4.2: Solution obtained with FDS + FDA-NCP (lines) and FDS+Newton's method (circles). Initial conditions are plotted in (a). Solutions at time $t = 0.008$ are shown in (b), (c) and (d) corresponding to grids with 51, 101 and 201 points.

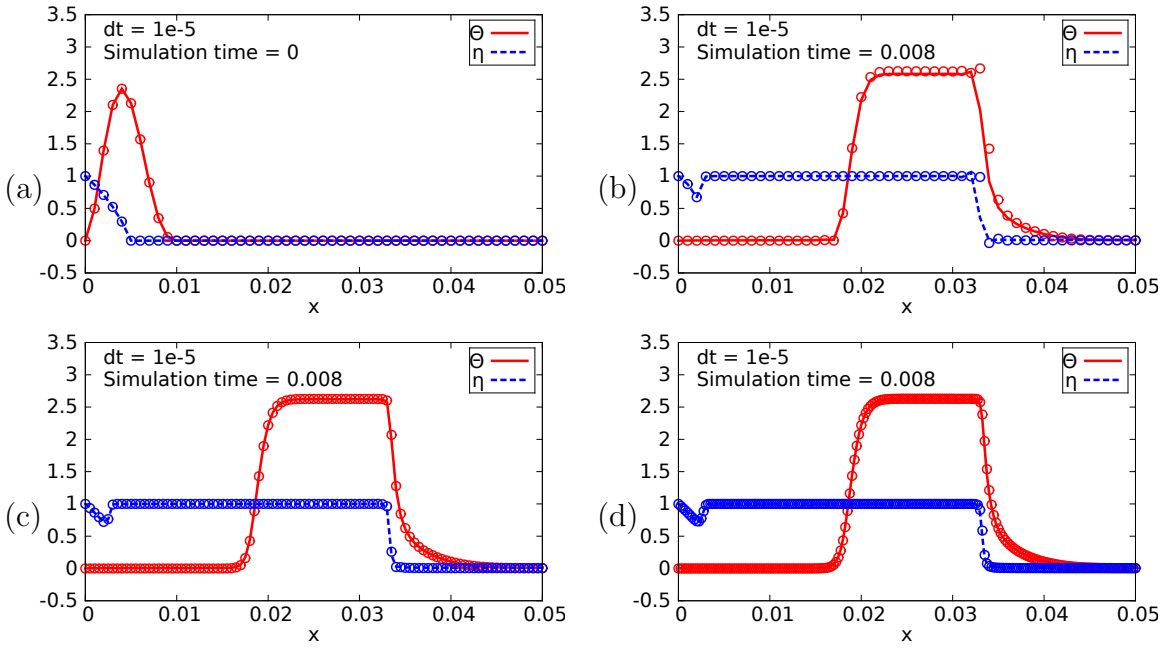

Figure 4.3: The solution obtained with FEM + FDA-NCP (lines) is compared to one obtained with FEM+Newton's method (circles). Initial conditions are plotted in (a). Solution at time $t = 0.008$ are shown in (b), (c) and (d) corresponding to grids with 51, 101 and 201 points.

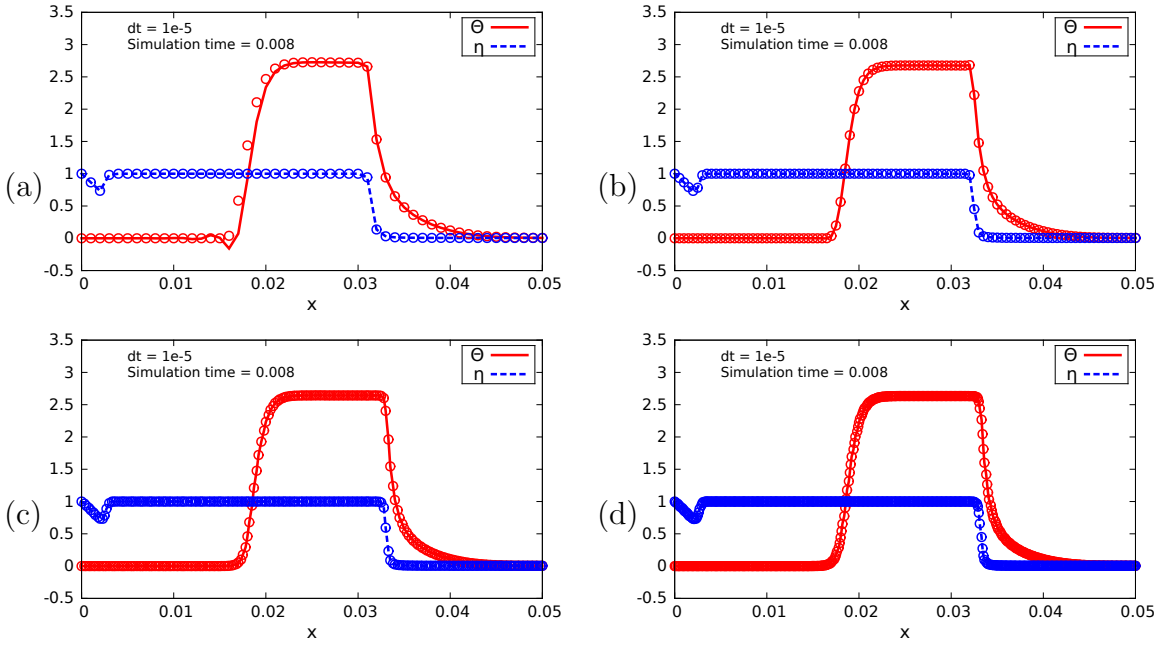

Figure 4.4: The solution obtained with FDS + Newton (lines) is compared to one obtained with FDS + FDA–MNCP (circles). Solutions at time $t = 0.008$ are shown in (a), (b), (c) and (d) corresponding to grids with 51, 101, 201 and 401 points.

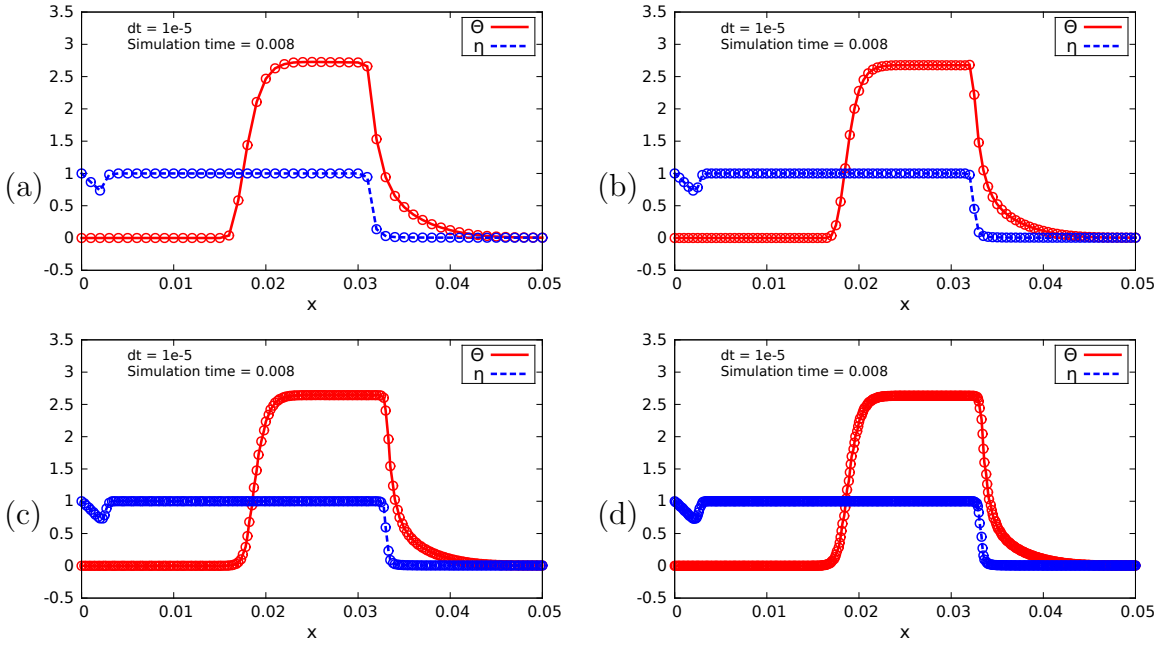

Figure 4.5: The solution obtained with FDS + FDA–NCP (lines) is compared to one obtained with FDS + FDA–MNCP (circles). Solutions at time $t = 0.008$ are shown in (a), (b), (c) and (d) corresponding to grids with 51, 101, 201 and 401 points.

4.2.1.3 Analysis of Riemann's problem

Apart of the combustion wave, the solution of System (1.5)-(1.6) possesses non-combustion waves, which can be studied analytically and used to validate numerical simulations. We consider a hyperbolic part of System (1.5)-(1.6) obtained by neglecting the reaction terms and second derivatives, see [42] and references therein. With this considerations we obtain the System (4.1).

$$\begin{aligned} &\frac{\partial \theta}{\partial t} + u\frac{\partial}{\partial x}\left(\frac{\theta_0 \theta}{\theta + \theta_0}\right) = 0, \\ &\frac{\partial \eta}{\partial t} = 0. \end{aligned} \tag{4.1}$$

The equations above form a system of conservation laws and can be solved for the corresponding Riemann problem, i.e., considering the initial data given by the discontinuous step function. Typically, the solution of a Riemann problem is a train of waves, which can be shocks, rarefaction or contact discontinuities. This solution is physically admissible if it satisfies the entropy conditions, see [69] for details.

Theorem 4.2.1. *The solution of System* (4.1) *with initial data given by*

$$(\theta(x,0), \eta(x,0)) = \begin{cases} (\theta_l, \eta_l), & x \leq 0 \\ (\theta_r, \eta_r), & x > 0 \end{cases} \tag{4.2}$$

where θ_l, η_l, θ_r and η_r are constants satisfying $\theta_l \leqslant \theta_r$ can contain:
(1) a Lax entropic contact wave satisfying $\theta_l = \theta_r$ and $\eta_r \geq 0$ with velocity equal to zero;
(2) a Lax entropic shock wave satisfying $\eta_l = \eta_r$ and $\theta_r \geq 0$ with velocity

$$s = \frac{u\theta_0^2}{(\theta_r + \theta_0)(\theta_l + \theta_0)}. \tag{4.3}$$

This theorem was proved in [12].

4.2.2 Model 2

For the model described in Section 1.2.2, following [12], the dimensionless parameter values are $\mathcal{E} = 93.8, \theta_0 = 3.67, V_T = 3.76$, $Pe = 1406, \lambda_Y = 0.001, V_Y = 5$, and $\mu_T = \mu_Y = \mu_\eta = 7.44 \times 10^{10}$.

4.2.2.1 Comparison of numerical results using FDA–MNCP

The numerical results obtained by FDS+FDA–MNCP and its validation with FDS + Newton's method are showed in Figure 4.6 (a), (b), (c) and (d). Over there can observed that the numerical results are very similar. Similar to Model 1, to validate our numerical solutions is used analytical estimative because we have not experimental data. In order is analyzed the Riemann's problem respective. This will be done in Section 4.2.2.2.

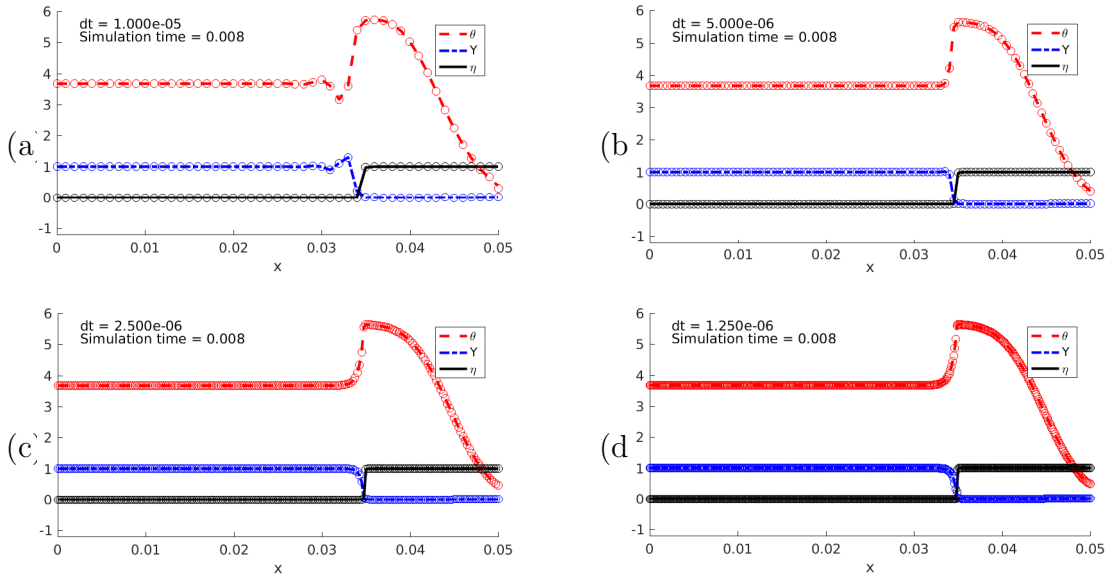

Figure 4.6: The solution obtained with FDS + Newton's method (lines) is compared to one obtained with FDS + FDA–MNCP (circles). Solutions at time $t = 0.008$ are shown in (a), (b), (c) and (d) corresponding to grids with $(\Delta x, \Delta t) = (10^{-3}, 10^{-5}), (0.5 \times 10^{-3}, 0.5 \times 10^{-5}), (0.25 \times 10^{-3}, 0.25 \times 10^{-5})$ and $(0.125 \times 10^{-3}, 0.125 \times 10^{-5})$.

4.2.2.2 Analysis of Riemann's problem

The numerical simulations are validated through comparison with analytical solution of the hyperbolic part of System (1.9)-(1.11). In order to study the non combustion waves it is assumed that $\Phi = 0$ and the diffusion coefficients are neglected in (1.9)-(1.11) corresponding to large time and large distances, see [41, 45] for more details.

Under these considerations the following system of equations is obtained

$$\frac{\partial \theta}{\partial t} + V_T \frac{\partial \theta}{\partial x} = 0, \tag{4.4}$$

$$\frac{\partial Y}{\partial t} + V_Y \frac{\partial Y}{\partial x} = 0, \tag{4.5}$$

$$\frac{\partial \eta}{\partial t} = 0. \tag{4.6}$$

Considering the initial data in the form of discontinuous step function for (4.4)–(4.6) is obtained a Riemann problem, which typically possesses a solution as a wave fans, that can be shocks, rarefaction or contact discontinuities. This solution is physically admissible if it satisfies the entropy conditions, see [69] for details.

In [12, 41, 45] the behavior the non combustion waves is studied as part of the solution of the Rieman's problem of the System (4.4)–(4.6). In the cited works it can verified that the Riemann problem possesses three non-combustion waves: The slowest one is an immobile fuel wave $V_\eta = 0$, the intermediate one is a thermal wave with speed V_T and the fastest one is the oxygen composition wave with speed V_Y, all these waves correspond to contact discontinuities.

Notice that the model given by System (1.9)–(1.12) is more general than those studied in [41, 70, 45, 44]. For the models presented in these papers it was proved that they possess a combustion wave in a form of a traveling wave solution. The proofs will not be presented here. Generally it was established the existence of combustion traveling waves classified as fast combustion waves, intermediate combustion waves and slow combustion waves. In the intermediate combustion wave and in the fast combustion wave the heat produced by combustion stays behind the combustion front. In the slow combustion wave the thermal wave goes in front of the combustion wave, which is the case of the simulation presented in Figure 4.6.

4.3 Elastic–plastic torsion problem

The exact solution of the Elastic–Plastic Torsion Problem of the cylindrical bar with cross-section $\Sigma \subset \mathbb{R}^2$ is known [10]:

$$\text{If } \theta \leq 2R \qquad \phi(x_1, x_2) = \theta(R^2 - r^2)/4,$$
$$\text{if } \theta \geq 2R \qquad \phi(x_1, x_2) = \begin{cases} R - r, & \text{if } \; R' \leq r \leq R, \\ -\theta\, r^2/4 + (R - 1/\theta), & \text{if } \; 0 \leq r \leq R', \end{cases} \tag{4.7}$$

where $\Sigma = \{(x_1, x_2) \in \mathbb{R}^2 \,/\, x_1^2 + x_2^2 \leq R^2\}$, $r = \sqrt{x_1^2 + x_2^2}$ and $R' = 2/\theta$.

4.3.1 Comparison of numerical results

The results are presented in Table 4.2. They are similar to the results presented in [11] summarized in Table 4.1, where the same problem is solved in the form of Def. 3.1.2. Notice that the number of mesh nodes is different.

Table 4.1: Number of iterations solving the Elastic–Plastic Torsion Problem presented in [11]. The total numbers of nodes is n.

n	143	537	2081	8193
Interior point	27	23	20	19

Table 4.2 shows the l_2 error of FDA–MNCP when compared to the exact solution (4.7). It can be observed that it is decreasing according to theoretical predictions until the numerical precision is reached in the last four columns. Notice that in the last three columns the total number of iterations stabilize for both values of the parameter β.

Table 4.2: Number of iterations solving the Elastic–Plastic Torsion Problem by FDA–MNCP. Numbers of total nodes is n.

$\beta \setminus n$		11	16	56	208	776	2798	3767	5358
1.1	FDA	17	17	17	20	25	31	30	32
	l_2 error	0.6885	0.3143	0.0791	0.0136	0.0049	0.0059	0.0022	0.0019
2.0	FDA	15	17	17	20	20	25	26	26
	l_2 error	0.6885	0.3143	0.0791	0.0136	0.0049	0.0059	0.0022	0.0019

In Figure 4.7 we show the comparison between the exact solution (4.7) and the numerical solution obtained by using FDA–MNCP with FEM. In agreement with the results presented in Table 4.2, the graphics are indistinguishable for big mesh numbers.

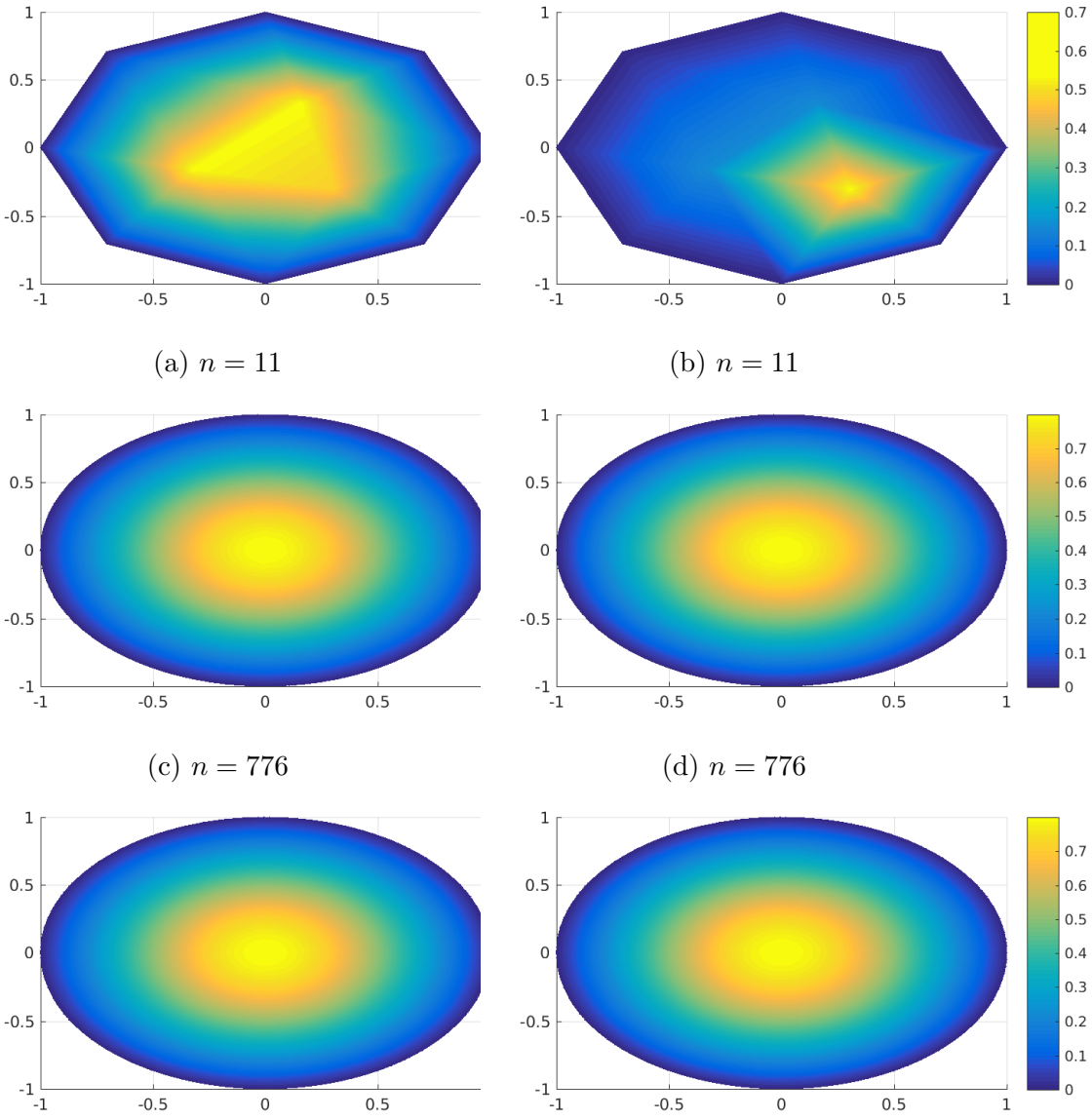

(a) $n = 11$ (b) $n = 11$

(c) $n = 776$ (d) $n = 776$

(e) $n = 5358$ (f) $n = 5358$

Figure 4.7: Exact (a, c and e) and numerical (b, d and f) solutions obtained for different mesh sizes n. The numerical simulations using FDA–MNCP for $\theta = 5$ and $R = 1$, [57].

Chapter 5

CONCLUSIONS

The Feasible Directions Algorithm for Mixed Nonlinear Complementarity Problems was investigated. It generalizes the ideas of FDA-NCP [24, 12]. Global and asymptotic convergence was rigorously proven. For the parameter $\beta \in]1, 2[$ the superlinear convergence was proved. On the other hand if $\beta = 2$ quadratic convergence was obtained.

The choice of the starting point should not be a problem for the algorithm as we proved the global convergence, i.e., for all starting points in the interior of the domain. This theoretical results were endorsed by numerical simulations with, at least, 10 different initial values for each benchmark problem. The Maratos effect was rarely observed in the test problems.

The FDA-MNCP is a simple, efficient and robust algorithm for mixed nonlinear complementarity problems and it converged for all test problems. As can be observed from the number of iterations required to solve the benchmark problems, it is robust in the sense that it does not need parameters tuning. In our case all the examples were solved using the same parameters μ, ν and β showing good results.

The main advantage in using the FDA–MNCP is the fact that the moving boundary is obtained directly as a solution of the mixed complementarity problem. This approach has a potential advantage over the Newton's method where the moving boundary

is difficult to obtain due to discontinuities of the solution. Another advantage of FDA–MNCP is that solution can be obtained with less points than the Newton's method.

We apply FDA–NCP and FDA–MNCP to different examples. The Oxygen Diffusion Problem is addressed in many works. Our results plotted on Figure 4.1 show good agreement with the literature.

The first In-Situ Combustion Model was formulated using mixed nonlinear complementarity problem with moving boundary, which can be an interesting approach for general flow in porous medium. Our numerical results show good agreement with direct numerical simulations using Newton's method as shown in Figure 4.4. They are almost identical to FDA–NCP as shown in Figure 4.5, Figure 4.2 and Figure 4.3. The numerical solutions for non–combustion waves that were obtained by FDA–MNCP are in agreement with the analytical results showed in Section 4.2.1.3 and Theorem 4.2.1.

The algorithm was tested using a second In Situ Combustion Model consisting of a system of three nonlinear partial differential equations. This model can be written as a nonlinear complementarity or as a mixed nonlinear complementarity problem. The numerical solutions for non–combustion waves that were obtained by FDA–MNCP are in agreement with the analytical results showed in Section 4.2.2.2. When solving it as NCP, the algorithm does no converge because of strong nonlinearities present in the model. Although, when written as MNCP, Feasible Direction Algorithm shows good results evidencing the advantages of FDA-MNCP. It converged for all time steps when applied for In Situ Combustion Model presented here.

The algorithm was applied to Elastic–Plastic Torsion Problem with a circular cross section. The obtained results agree with the analytical solution and with the ones found in the literature. Proving the Hypothesis 3.3.1–3.3.4 is not easy and they not are proved explicitly. It is assumed that the studied models satisfy all conditions.

These results can also be extended to other problems, such as, Mathematical Program with Equilibrium Constraints (MPEC).

One possibility for the future work is to investigate the algorithm for the case when the matrix $\nabla S(x, y)$ is singular.

Bibliography

[1] Ferris, M.C., Pang, J.S.: Engineering and economic applications of complementarity problems. Siam Review **39**(4), 669–713 (1997)

[2] Dirkse, S., Ferris, M.: Mcplib: A collection of nonlinear mixed complementarity problems. Optimization Methods and Software **5**(4), 319–345 (1995)

[3] Zukeyama Perea, Y.Y.: Implementación de una unidad de delayed coking como mejora de los rendimientos y optimización del fraccionamiento de crudo pesado. Programa Cybertesis PERÚ (2009). Universidad Nacional de Ingeniería

[4] Chapiro, G.: Gas-solid combustion in insulated porous media. Ph.D. thesis, IMPA (2009)

[5] Rubinstein, R.: On the elastic-plastic torsion problem. Journal of Engineering Mathematics **11**(4), 319–323 (1977)

[6] Idone, G., Maugeri, A., Vitanza, C.: Variational inequalities and the elastic-plastic torsion problem. Journal of Optimization Theory and Applications **117**(3), 489–501 (2003)

[7] Facchinei, F., Pang, J.S.: Finite-dimensional variational inequalities and complementarity problems, vol. 1. Springer Science & Business Media (2003)

[8] Herakovich, C.T., Hodge, P.G.: Elastic-plastic torsion of hollow bars by quadratic programming. International Journal of Mechanical Sciences **11**(1), 53–63 (1969)

[9] Leontiev, A., Huacasi, W., Herskovits, J.: An optimization technique for the solution of the signorini problem using the boundary element method. Structural and Multidisciplinary Optimization **24**(1), 72–77 (2002)

[10] Glowinski, R., Lions, J.L., Trémolières, R., Lions, J.L.: Numerical analysis of variational inequalities, vol. 8. North-Holland Amsterdam (1981)

[11] Judice, J., Soares, M.: Solution of some linear complementarity problems arising in variational models of mechanics. Investigaç. Operac. **18**, 17–31 (1998)

[12] Chapiro, G., Ramírez, A., Herskovits, J., Mazorche, S., Pereira, W.: Numerical solution of a class of moving boundary problems with a nonlinear complementarity approach. Journal of Optimization Theory and Applications **168**(2), 534–550 (2016)

[13] Ramírez A.; Mazorche, S., Chapiro, G.: Numerical simulation of an in-situ combustion model formulated as mixed complementarity problem. Revista Interdisciplinar de Pesquisa em Engenharia - RIPE **2**(17), 172–181 (2016)

[14] Simantiraki, E., Shanno, D.F.: An infeasible-interior-point algorithm for solving mixed complementarity problems. Complementarity and Variational Problems: State of the Art. pp. 386–404 (1997)

[15] Dirkse, S., Ferris, M.: The path solver: a nommonotone stabilization scheme for mixed complementarity problems. Optimization Methods and Software **5**(2), 123–156 (1995)

[16] Daryina, A.N., Izmailov, A.F., Solodov, M.V.: A class of active-set newton methods for mixed complementarityproblems. SIAM Journal on Optimization **15**(2), 409–429 (2005)

[17] Daryina, A., Izmailov, A., Solodov, M.: Numerical results for a globalized active-set newton method for mixed complementarity problems. Computational & Applied Mathematics **24**(2), 293–316 (2005)

[18] Liu, C.S., Atluri, S.N.: A fictitious time integration method (ftim) for solving mixed complementarity problems with applications to non-linear optimization. CMES: Computer Modeling in Engineering & Sciences **34**(2), 155–178 (2008)

[19] Gabriel, S.A.: A hybrid smoothing method for mixed nonlinear complementarity problems. Computational Optimization and Applications **9**(2), 153–173 (1998)

[20] Kanzow, C.: Global optimization techniques for mixed complementarity problems. Journal of Global Optimization **16**(1), 1–21 (2000)

[21] Herskovits, J.: A feasible direction interior-point technique for nonlinear optimization. Journal of optimization theory and applications **99**(1), 121–146 (1998)

[22] Herskovits, J.: A two-stage feasible directions algorithm for nonlinear constrained optimization. Mathematical Programming **36**(1), 19–38 (1986)

[23] Herskovits, J.: A two-stage feasible direction algorithm including variable metric techniques for non-linear optimization problems. Ph.D. thesis, Inria (1982)

[24] Herskovits, J., Mazorche, S.R.: A feasible directions algorithm for nonlinear complementarity problems and applications in mechanics. Structural and Multidisciplinary Optimization **37**(5), 435–446 (2009)

[25] Mazorche, S.R.: Algoritmos para problemas de complementaridade não linear. Ph.D. thesis, Universidade Federal do Rio de Janeiro (2007)

[26] Crank, J., Gupta, R.: A moving boundary problem arising from the diffusion of oxygen in absorbing tissue. IMA Journal of Applied Mathematics **10**(1), 19–33 (1972)

[27] Strikwerda, J.C.: Finite difference schemes and partial differential equations. SIAM (2004)

[28] Johnson, C.: Numerical solution of partial differential equations by the finite element method. Courier Corporation (2012)

[29] Crank, J.: Free and moving boundary problems. Oxford University Press (1987)

[30] Gupta, R., Kumar, D.: Variable time step methods for one-dimensional stefan problem with mixed boundary condition. International Journal of Heat and Mass Transfer **24**(2), 251–259 (1981)

[31] Ahmed, S.: A numerical method for oxygen diffusion and absorption in a sike cell. Applied mathematics and computation **173**(1), 668–682 (2006)

[32] Boureghda, A.: Numerical solution of the oxygen diffusion in absorbing tissue with a moving boundary. International Journal for Numerical Methods in Biomedical Engineering **22**(9), 933–942 (2006)

[33] Çatal, S.: Numerical approximation for the oxygen diffusion problem. Applied mathematics and computation **145**(2), 361–369 (2003)

[34] Gupta, R.S., Banik, N.: Approximate method for the oxygen diffusion problem. International Journal of Heat and Mass Transfer **32**(4), 781–783 (1989)

[35] Hansen, E., Hougaard, P.: On a moving boundary problem from biomechanics. IMA Journal of Applied Mathematics **13**(3), 385–398 (1974)

[36] Chapiro, G., Mazorche, S., Herskovits, J., Roche, J.: Solution of the nonlinear parabolic problems using nonlinear complementarity algorithm (fda-ncp). Mecánica Computacional **29**(21), 2141–2153 (2010)

[37] Pereira, W., Ramírez, A., Mazorche, S., Chapiro, G.: Simulação de um problema de difusão de oxigênio utilizando o método de elementos finitos e fda-ncp. XI Simpósio de Mecânica Computacional/II Encontro Mineiro de Modelagem Computacional (2014)

[38] Ramírez G., A.: Aplicação do método de complementaridade não linear para o estudo de combustão de oxigênio in situ. Master's thesis, Universidade Federal de Juiz de Fora (2013)

[39] Chapiro, G., Hime, G., Marchesin, D.: Simulaçao de ondas de combustao gás-sólido em meios porosos. Congresso Nacional de Matemática Aplicada e Computacional 2008 (2008)

[40] Andonaire, P., Francisco, C.: Alternativas para la explotación de crudo pesado en la selva norte de perú-propuesta para un desarrollo integral estado/contratista (2006)

[41] Chapiro, G., Marchesin, D., Schecter, S.: Combustion waves and riemann solutions in light porous foam. Journal of Hyperbolic Differential Equations **11**(02), 295–328 (2014)

[42] Chapiro, G., Mailybaev, A., de Souza, A., Marchesin, D., Bruining, J.: Asymptotic approximation of long-time solution for low-temperature filtration combustion. Computational geosciences **16**(3), 799–808 (2012)

[43] Akkutlu, I., Yortsos, Y.: The dynamics of in-situ combustion fronts in porous media. Combustion and Flame **134**(3), 229–247 (2003)

[44] Chapiro, G., Senos, L.: Riemann solutions for counterflow combustion in light porous foam. Computational and Applied Mathematics pp. 1–16 (2017)

[45] Fathid, O., Schecter, S., Chapiro, G.: Travelling waves in a simplified gas–solid combustion model in porous media. To appear in Adv. in Dif. Eq. (2018)

[46] Wagner, W., Gruttmann, F.: Finite element analysis of saint–venant torsion problem with exact integration of the elastic–plastic constitutive equations. Computer methods in applied mechanics and engineering **190**(29), 3831–3848 (2001)

[47] Mendelson, A.: Elastic-plastic torsion problem for strain-hardening materials. Nasa Technical Note. National Aeronautics and Space Administration (1968)

[48] Lubliner, J.: Plasticity theory. Courier Corporation (2008)

[49] Satake, A., Reddy, J.: A numerical method for elastic-plastic torsion by variational inequality. International Journal of Solids and Structures **16**(1), 1–18 (1980)

[50] Herskovits, J., Mazorche, S.R.: A new interior point algorithm for nonlinear complementarily problems. In: 6th WCSMO–World Congress on Structural and Multidisciplinary Optimization (2005)

[51] Gharbia, I.B., Jaffré, J.: Gas phase appearance and disappearance as a problem with complementarity constraints. Mathematics and Computers in Simulation **99**, 28–36 (2014)

[52] Chen, C., Mangasarian, O.L.: A class of smoothing functions for nonlinear and mixed complementarity problems. Computational Optimization and Applications **5**(2), 97–138 (1996)

[53] Lauser, A., Hager, C., Helmig, R., Wohlmuth, B.: A new approach for phase transitions in miscible multi-phase flow in porous media. Advances in Water Resources **34**(8), 957–966 (2011)

[54] Gupta, S.C.: The classical Stefan problem: basic concepts, modelling and analysis, vol. 45. Elsevier (2003)

[55] Baiocchi, C., Capelo, A.C.: Variational and quasivariational inequalities: Applications to free boundary problems. John Wiley & Sons, INC., 605 Third Ave., New York, NY 10158, USA, 400 (1984)

[56] Baiocchi, C., Pozzi, G.: An evolution variational inequality related to a diffusion-absorption problem. Applied Mathematics & Optimization **2**(4), 304–314 (1975)

[57] Ramírez, A., Mazorche, S., Herskovits, J., Chapiro, G.: An interior point algorithm for mixed complementarity nonlinear problems. Journal of Optimization Theory and Applications **175**(2), 432–449 (2017)

[58] Billups, S.C., Dirkse, S.P., Ferris, M.C.: A comparison of large scale mixed complementarity problem solvers. Computational Optimization and Applications **7**(1), 3–25 (1997). DOI 10.1023/A:1008632215341

[59] McCormick, G.P.: Second Order Conditions for Constrained Minima, pp. 259–270. Springer Basel, Basel (2014)

[60] Bazaraa, M.S., Sherali, H.D., Shetty, C.M.: Nonlinear programming: theory and algorithms. John Wiley & Sons (2013)

[61] Gabriel, S.A.: Solving discretely constrained mixed complementarity problems using a median function. Optimization and Engineering pp. 1–28 (2017)

[62] Rheinboldt, W.: Some nonlinear test problems (2003). Available online: http:folk.uib.no/ssu029/Pdf_file/Testproblems/testprobRheinboldt03.pdf

[63] Sun, D., Han, J.: Newton and quasi-newton methods for a class of nonsmooth equations and related problems. SIAM Journal on Optimization **7**(2), 463–480 (1997)

[64] Kojima, M., Shindoh, S.: Extensions of Newton and quasi-Newton methods to systems of PC 1 equations. Inst. of Technology, Department of Information Sciences (1986)

[65] Stampacchia, G.: Formes bilinéaires coercitives sur les ensembles convexes. CR Acad. Sci. Paris **258**(1), 964 (1964)

[66] Brezis, H., Sibony, M.: Équivalence de deux inéquations variationnelles et applications. Archive for Rational Mechanics and Analysis **41**(4), 254–265 (1971)

[67] Morton, K.W., Mayers, D.F.: Numerical solution of partial differential equations: an introduction. Cambridge university press (2005)

[68] Bruining, J., Mailybaev, A.A., Marchesin, D.: Filtration combustion in wet porous medium. SIAM Journal on Applied Mathematics **70**(4), 1157–1177 (2009)

[69] LeVeque, R.J.: Numerical methods for conservation laws, vol. 132. Springer (1992)

[70] Chapiro, G., Marchesin, D.: The effect of thermal losses on traveling waves for in-situ combustion in porous medium. Journal of Physics: Conference Series **633**(1) (2015)

Appendix A

DISCRETIZATION OF IN SITU COMBUSTION MODELS

In this seccion is described briefly the finite diference esqueme of Crank–Nicolson for the in situ combustion models that were presented in Section 1.2 with the objetive of to obtain the discrete formulations for to apply the FDA–MNCP and Newton's method. The aproximation of derivatives considered are:

$$\partial_t w(x_m, t_{n+\frac{1}{2}}) = \frac{w_m^{n+1} - w_m^n}{k}, \tag{A.1a}$$

$$\partial_{xx} w(x_m, t_{n+\frac{1}{2}}) = \frac{w_{m+1}^{n+1} - 2w_m^{n+1} + w_{m-1}^{n+1}}{2h^2} + \frac{w_{m+1}^n - 2w_m^n + w_{m-1}^n}{2h^2}, \tag{A.1b}$$

$$\partial_x F(w(x_m, t_{n+\frac{1}{2}})) = \frac{F_{m+1}^{n+1} - F_{m-1}^{n+1}}{4h} + \frac{F_{m+1}^n - F_{m-1}^n}{4h}, \tag{A.1c}$$

$$\Phi(w(x_m, t_{n+\frac{1}{2}})) = \frac{\Phi_m^{n+1} + \Phi_m^n}{2}, \tag{A.1d}$$

where the values of h, k are as in Section 4.2. Same discretization was employed in [42, 41] to simulate more general and complex combustion models. Goods results were obtained when compared with analytical solutions.

A.1 Model 1

In this section consider the System 1.5–1.7 and are considered the constants defined bellow

$$H = \frac{1}{Pe}, \quad \lambda = \frac{k}{h}, \quad \mu = \frac{k}{h^2}. \tag{A.2}$$

The discrete formulation as NCP for this model can be found in [38].

A.1.1 Discrete formulation as MNCP

Let be $F(\theta, \eta)$ the differential operator corresponding to the left side of inequality (3.42) and $Q(\theta, \eta)$ the differential operator corresponding to the left side of equality (3.43). We write it in the discrete form as MNCP, using Crank-Nicolson scheme, thus we obtain these operatos in variables $(\theta^{n+1}, \eta^{n+1})$:

$$F(\theta^{n+1}, \eta^{n+1}) = A\theta^{n+1} + \lambda T(\theta^{n+1}) - 2k\Psi(\theta^{n+1}, \eta^{n+1}) - LD(\theta^n, \eta^n) \geq 0, \quad \text{(A.3)}$$

$$Q(\theta^{n+1}, \eta^{n+1}) = \eta^{n+1} - k\Psi^{n+1} - \left[\eta^n + \frac{k}{2}\Psi^n\right] = 0, \quad \text{(A.4)}$$

with complementarity condition

$$\theta^{n+1} \bullet F(\theta^{n+1}, \eta^{n+1}) = 0, \quad \text{(A.5)}$$

where $LD(\theta^n, \eta^n) = B\theta^n - \lambda T(\theta^n) + 2k\Psi(\theta^n, \eta^n) + UR$ is known in each instant of time. The matrices $A, B \in \mathbb{R}^{m\times m}$ and vectors $T, \Psi \in \mathbb{R}^{m\times 1}$ are:

$$A = \begin{pmatrix} (4+4\mu H) & -2\mu H & 0 & \cdots & 0 & 0 \\ -2\mu H & (4+4\mu H) & -2\mu H & & & 0 \\ 0 & -2\mu H & (4+4\mu H) & & & 0 \\ \vdots & & & \ddots & & \vdots \\ 0 & 0 & 0 & & (4+4\mu H) & -2\mu H \\ 0 & 0 & 0 & \cdots & -4\mu H & (4+4\mu H) \end{pmatrix}, \quad \text{(A.6)}$$

$$B = \begin{pmatrix} (4-4\mu H) & 2\mu H & 0 & \cdots & 0 & 0 \\ 2\mu H & (4-4\mu H) & 2\mu H & & 0 & 0 \\ 0 & 2\mu H & (4-4\mu H) & & 0 & 0 \\ \vdots & & & \ddots & & \vdots \\ 0 & 0 & 0 & & (4-4\mu H) & 2\mu H \\ 0 & 0 & 0 & \cdots & 4\mu H & (4-4\mu H) \end{pmatrix}, \tag{A.7}$$

$$T^n = T(\theta^n) = \begin{pmatrix} G_2^n - G_0^n \\ G_3^n - G_1^n \\ G_4^n - G_2^n \\ \vdots \\ G_M^n - G_{M-2}^n \\ 0 \end{pmatrix}, \quad \Psi^n = \Psi(\theta^n, \eta^n) = \begin{pmatrix} \Phi_1^n \\ \Phi_2^n \\ \Phi_3^n \\ \vdots \\ \Phi_{M-1}^n \\ \Phi_M^n \end{pmatrix}, \tag{A.8}$$

$$UR = \begin{pmatrix} 4\mu H\theta_0^n \\ 0 \\ 0 \\ \vdots \\ 0 \\ 0 \end{pmatrix}. \tag{A.9}$$

A.1.2 Discrete formulation as nonlinear system of equations

We write the System (1.5)-(1.6) in the discrete form as nonlinear system of equations, using Crank-Nicolson scheme, thus we obtain these operatos in variables $(\theta^{n+1}, \eta^{n+1})$:

$$G(\theta^{n+1}, \eta^{n+1}) = \begin{bmatrix} A\theta^{n+1} + \lambda T(\theta^{n+1}) - 2k\Psi(\theta^{n+1}, \eta^{n+1}) - LD(\theta^n, \eta^n) \\ \eta^{n+1} - k\Psi^{n+1} - \left[\eta^n + \frac{k}{2}\Psi^n\right] \end{bmatrix} = 0, \tag{A.10}$$

where the matrices $A, B \in \mathbb{R}^{m\times m}$ and vectors $T, \Psi \in \mathbb{R}^{m\times 1}$ are the same of Section A.1.1.

A.2 Model 2

We obtain the discrete formulation of System 1.9–1.11.

A.2.1 Discrete formulation as MNCP

Let be $F(\theta, Y, \eta)$ the differential operator corresponding to the left side of equality (3.45) and $Q(\theta, Y, \eta)$ the differential operator corresponding to the left side of inequalities (3.46)–(3.47). We write it in the discrete form as MNCP, using Crank-Nicolson scheme, thus we obtain these operators in variables $x = \theta^{n+1} \in \mathbb{R}_+^M, \quad y = (Y^{n+1}, \eta^{n+1}) \in \mathbb{R}^M \times \mathbb{R}^M$:

$$F_\Delta(x, y) = -(\alpha_1 + \alpha_2)\theta_{m-1}^{n+1} + (1 + 2\alpha_2)\theta_m^{n+1} + (\alpha_1 - \alpha_2)\theta_{m+1}^{n+1} - \alpha_3\Phi_m^{n+1} - RHS_{1,m}^n,$$

$$Q_\Delta(x, y) = \begin{bmatrix} LHS_m^{n+1} - RHS_{2,m}^n \\ \\ \eta_m^{n+1} + \gamma_1\Phi_m^{n+1} - RHS_{3,m}^n \end{bmatrix},$$

where

$$LHS_m^{n+1} = -(\beta_1 + \beta_2)Y_{m-1}^{n+1} + (1 + 2\beta_2)Y_m^{n+1} + (\beta_1 - \beta_2)Y_{m+1}^{n+1} - \beta_3\Phi_m^{n+1}$$

$$RHS_{1,m}^n = (\alpha_1 + \alpha_2)\theta_{m-1}^n + (1 - 2\alpha_2)\theta_m^n - (\alpha_1 - \alpha_2)\theta_{m+1}^n + \alpha_3\Phi_m^n,$$

$$RHS_{2,m}^n = (\beta_1 + \beta_2)\theta_{m-1}^n + (1 - 2\beta_2)\theta_m^n - (\beta_1 - \beta_2)\theta_{m+1}^n - \beta_3\Phi_m^n,$$

$$RHS_{3,m}^n = \eta_m^n - \gamma_1\Phi_m^n,$$

$$\Phi_m^n = Y_m^n\,\eta_m^n\,exp(-\xi/(\theta_m^n + \theta_0)),$$

and

$$\begin{aligned} &\alpha_1 = \frac{V_T\,\Delta t}{4h}, \quad \alpha_2 = \frac{\lambda_T\,\Delta t}{2h^2}, \quad \alpha_3 = \frac{\mu_T\,\Delta t}{2}, \quad \beta_1 = \frac{V_Y\,\Delta t}{4h}, \\ &\beta_2 = \frac{\lambda_Y\,\Delta t}{2h^2}, \quad \beta_3 = \frac{\mu_Y\,\Delta t}{2}, \quad \gamma_1 = \frac{\mu_\eta\,\Delta t}{2}. \end{aligned} \tag{A.11}$$

Substituting the differential operator $F(\theta, \eta)$ in (3.44) by the discrete operator $F_\Delta(\theta, \eta)$ and isolating the terms for time step $n+1$ on the left, we obtain the system of equations describing time evolution. The evaluation equation for the grid points $m = 0$

and $m = M$ can be described using the boundary conditions. The boundary conditions impose constant temperature and no fuel at the left end of the interval, $x_0 = 0$. That is $\theta(x_0, t) = 0, Y(x_0, t) = 0$ and $\eta(x_0, t) = 0$, $t \geq 0$. As there is no fixed right point, the boundary conditions at the right are modeled as zero flow Neumann boundary conditions. Thus, it is considering h, k as Section 4.2 is obtained the discrete formulation as MNCP

$$F(x, y) = A\theta^{n+1} - \alpha_3\Psi^{n+1} - [B\theta^n + \alpha_3\Psi^n + Fr_\theta] \geq 0, \tag{A.12}$$

$$Q(x, y) = \begin{bmatrix} RY^{n+1} + \beta_3\Psi^{n+1} - [SY^n - \beta_3\Psi^n + Fr_Y] \\ \\ \eta^{n+1} + \gamma_1\Psi^{n+1} - [\eta^n - \gamma_1\Psi^n] \end{bmatrix} = 0. \tag{A.13}$$

with complementarity condition

$$\theta^{n+1} \bullet F(\theta^{n+1}, Y^{n+1}, \eta^{n+1}) = 0, \tag{A.14}$$

where $x = \theta^{n+1} \in \mathbb{R}^M_+$, $\quad y = (Y^{n+1}, \eta^{n+1}) \in \mathbb{R}^M \times \mathbb{R}^M$,. The matrices $A, B, R, S \in \mathbb{R}^{M\times M}$ and vetors $\Psi^n, Fr_Y, Fr_\theta \in \mathbb{R}^M$ are showed bellow and for more details see [38].

$$A = \begin{bmatrix} (1+2\alpha_2) & (\alpha_1-\alpha_2) & 0 & \cdots & 0 & 0 \\ -(\alpha_1+\alpha_2) & (1+2\alpha_2) & (\alpha_1-\alpha_2) & & 0 & 0 \\ 0 & -(\alpha_1+\alpha_2) & (1+2\alpha_2) & & 0 & 0 \\ \\ \vdots & & & \ddots & & \vdots \\ \\ 0 & 0 & 0 & & (1+2\alpha_2) & (\alpha_1-\alpha_2) \\ 0 & 0 & 0 & \cdots & -2\alpha_2 & (1+2\alpha_2) \end{bmatrix},$$

$$B = \begin{bmatrix} (1-2\alpha_2) & -(\alpha_1-\alpha_2) & 0 & \cdots & 0 & 0 \\ (\alpha_1+\alpha_2) & (1-2\alpha_2) & -(\alpha_1-\alpha_2) & & 0 & 0 \\ 0 & (\alpha_1+\alpha_2) & (1+2\alpha_2) & & 0 & 0 \\ \vdots & & & \ddots & & \vdots \\ 0 & 0 & 0 & & (1+2\alpha_2) & -(\alpha_1-\alpha_2) \\ 0 & 0 & 0 & \cdots & 2\alpha_2 & (1+2\alpha_2) \end{bmatrix},$$

$$R = \begin{bmatrix} (1+2\beta_2) & (\beta_1-\beta_2) & 0 & \cdots & 0 & 0 \\ -(\beta_1+\beta_2) & (1+2\beta_2) & (\beta_1-\beta_2) & & 0 & 0 \\ 0 & -(\beta_1+\beta_2) & (1+2\beta_2) & & 0 & 0 \\ \vdots & & & \ddots & & \vdots \\ 0 & 0 & 0 & & (1+2\beta_2) & (\beta_1-\beta_2) \\ 0 & 0 & 0 & \cdots & -2\beta_2 & (1+2\beta_2) \end{bmatrix},$$

$$S = \begin{bmatrix} (1-2\beta_2) & -(\beta_1-\beta_2) & 0 & \cdots & 0 & 0 \\ (\beta_1+\beta_2) & (1-2\beta_2) & -(\beta_1-\beta_2) & & 0 & 0 \\ 0 & (\beta_1+\beta_2) & (1+2\beta_2) & & 0 & 0 \\ \vdots & & & \ddots & & \vdots \\ 0 & 0 & 0 & & (1-2\beta_2) & -(\beta_1-\beta_2) \\ 0 & 0 & 0 & \cdots & 2\beta_2 & (1-2\beta_2) \end{bmatrix},$$

$$\Psi^n = \begin{bmatrix} \Phi_1^n \\ \Phi_2^n \\ \Phi_3^n \\ \vdots \\ \Phi_{M-1}^n \\ \Phi_M^n \end{bmatrix}, \quad Fr_\theta = \begin{bmatrix} 2(\alpha_1+\alpha_2)\theta_L \\ 0 \\ 0 \\ \vdots \\ 0 \\ 0 \end{bmatrix}, \quad Fr_Y = \begin{bmatrix} 2(\beta_1+\beta_2)Y_L \\ 0 \\ 0 \\ \vdots \\ 0 \\ 0 \end{bmatrix}.$$

Joining (A.12), (A.13) and (A.14) is obtained the formulation as MNCP, which can be resolved by FDA–MNCP described in Section 3.2.

A.2.2 Discrete formulation as nonlinear system of equations

System (1.9)-(1.11) can be written in the discrete form by using Crank-Nicolson scheme:

$$G(\theta^{n+1}, Y^{n+1}, \eta^{n+1}) = \begin{pmatrix} A\theta^{n+1} - \alpha_3\Psi^{n+1} - [B\theta^n + \alpha_3\Psi^n + Fr_\theta] \\ RY^{n+1} + \beta_3\Psi^{n+1} - [SY^n - \beta_3\Psi^n + Fr_Y] \\ \eta^{n+1} + \gamma_1\Psi^{n+1} - [\eta^n - \gamma_1\Psi^n] \end{pmatrix} = 0, \quad \text{(A.15)}$$

where the matrices A, B, R, S, the vectors Ψ^n, Fr_θ, Fr_Y and constants α_1, α_2, α_3, β_1, β_2, β_3 and γ_1 are the same as in Section A.2.1. Equation $G(\theta^{n+1}, Y^{n+1}, \eta^{n+1}) = 0$, where G is given by A.15 is solved by Newton's method.

For discrete formulation as NCP of System (1.9)-(1.11), it is written as

$$G(\theta^{n+1}, Y^{n+1}, \eta^{n+1}) \geq 0, \quad \text{(A.16)}$$

where function G is given by A.15.